Food Bioscience 71 (2025) 107412

Contents lists available at ScienceDirect

Food Bioscience

journal homepage: www.elsevier.com/locate/fbio

Structural-taste relationship and molecular interaction mechanisms of umami peptides from *Meretrix lyrata* hydrolysates: Insights into key binding sites and thermodynamic drivers

Chunyong Song [a,b], Rong Jiang [a,b], Mingtang Tan [a,b], Zhongqin Chen [a,b], Huina Zheng [a,b], Jialong Gao [a,b], Haisheng Lin [a,b], Wenhong Cao [a,b,*]

[a] Shenzhen Institute of Guangdong Ocean University, Shenzhen, 518108, China
[b] College of Food Science and Technology, Guangdong Ocean University, National Research and Development Branch Center for Shellfish Processing (Zhanjiang), Guangdong Provincial Key Laboratory of Aquatic Products Processing and Safety, Zhanjiang, 524088, China

ARTICLE INFO

Keywords:
Meretrix lyrata
Umami peptides
Umami receptor
Molecular docking
Key binding sites
Thermodynamic interactions

ABSTRACT

To systematically investigate the umami mechanism of umami peptides, 224 umami peptides were rapidly screened from *Meretrix lyrata* hydrolysates based on peptidomics and molecular docking. Subsequently, four umami peptides (TWDLL, EDFLLA, VDEVLRL, and LALDWLAR) were synthesized for further exploring interactions with umami receptor following their microstructure, thermodynamic characterization, and umami characteristics. The results revealed that 224 umami peptides were significantly enriched in Leu, Val, Asp, and Glu residues, with hydrophobic/alkaline amino acid residues at terminal positions. Furthermore, umami peptides could notably alter umami receptor's surface morphology, evidenced by increased surface roughness, and their interaction was primarily mediated by hydrogen and hydrophobic bonds, with an average binding energy of −7.4 kcal/mol. Specifically, the key binding sites were identified as residues of Leu51, Ser107, Ser109, Asp243, and Ile244 in the T1R1 subunit, along with residues of Leu173, Glu217, Arg220, Ser224, and Glu240 in the T1R3 subunit. Similar to monosodium glutamate (MSG), four umami peptides demonstrated strong-affinity interaction with the umami receptor, with binding affinity constants (*Kd*) ranging from 5.440×10^{-9} to 4.653×10^{-8} M. Moreover, three umami peptides (TWDLL, EDFLLA, and VDEVLRL) exhibited exceptional umami taste, equivalent to MSG at 47 % of the same concentration. These findings establish structure-taste relationships governing umami peptide-receptor recognition.

1. Introduction

Umami, recognized as the fifth fundamental taste alongside sweet, sour, bitter, and salty sensations, is mediated by a diverse array of umami-active compounds (Song, Wang et al., 2025; Yang et al., 2024). These compounds, encompassing glutamates, flavor-enhancing nucleotides, and bioactive peptides, synergistically contribute to flavor enhancement by imparting palatability to food products (Lee et al., 2025; Song et al., 2024). Monosodium glutamate (MSG) has served as a fundamental flavor enhancer in food applications for over a century (Guo, Yu et al., 2024). Nevertheless, its widespread utilization has sparked ongoing scientific debate concerning potential health implications, prompting increased scrutiny regarding its dietary safety profile. Besides, the excessive consumption of sodium salt has caused a severe global public health crisis, with global sodium intake averaging between 3.54 and 4.72 g/day-substantially exceeding the World Health Organization's (WHO) recommended daily limit of 2.0 g/day (Le et al., 2022; Wang et al., 2023). Over 60 % of individuals in the United States also

Abbreviations: (MSG), Monosodium glutamate; (WHO), World health organization; (GPCRs), G-protein-coupled receptors; (VFTD), Venus flytrap domain; (3D), Three-dimensional; (PBS), Phosphate buffer solution; (LC), Liquid chromatography; (DS), Discovery Studio; (AARs), Amino acid residues; (GRAVY), Grand average of hydropathicity; (AFM), Atomic force microscopy; (ITC), Isothermal titration calorimetry; (CTO), Cross-selective taste oscillation; (AAE), Autonomous array electrode; (QDA), Quantitative descriptive analysis; (PCA), Principal component analysis.

* Corresponding author. College of Food Science and Technology, Guangdong Ocean University, Zhanjiang 524088, China; No.1 Haida Road, Zhanjiang, 524088, China.
E-mail address: cwenhong@gdou.edu.cn (W. Cao).

https://doi.org/10.1016/j.fbio.2025.107412
Received 27 May 2025; Received in revised form 12 August 2025; Accepted 13 August 2025
Available online 13 August 2025

claim reluctance to purchase food products containing MSG (Hiranpradith et al., 2023). As a result, the food industry is confronted with the dual challenge of replacing MSG in food without sacrificing its distinct umami flavor.

The umami peptides have drawn attention for their safe, nutritious, and sustainable characteristics, along with their capacity to reduce MSG and salt consumption (Song, Wang et al., 2025; Wang et al., 2023). These peptides, typically oligomeric and molecular weights below 3000 Da, interact with umami receptors on human taste buds to generate their unique umami taste profile (Song, Wang et al., 2025; Yang et al., 2024). At present, the primary umami receptors identified include the heterodimer T1R1/T1R3 and the taste-type metabotropic glutamate receptors mGluR1 and mGluR4, which play a specific role in recognizing L-glutamate and L-aspartate (Chang et al., 2024; Song, Wang et al., 2025; Yu et al., 2024). The T1R1/T1R3 receptor is a G-protein-coupled receptor (GPCRs) that acts as a heterodimer, formed by the association of two distinct GPCR subunits (Chang et al., 2024; Song, Wang et al., 2025). When umami peptides bind to a specific region within the extracellular venus flytrap domain (VFTD), the T1R1/T1R3 receptor becomes activated and its structure transitions to an active conformation, thereby allowing the brain to perceive umami tastes (Song, Wang et al., 2025; Yang et al., 2021; Yao et al., 2024). Subsequently, a variety of umami peptides were screened from tempeh (Indonesian fermented soybean) (Amin et al., 2020), fermented grains (Han et al., 2024), *Agaricus bisporus* and *Volvariella volvacea* (Li et al., 2025), high-umami scored air-dried chicken (Yu et al., 2024), and other protein hydrolysates (Chang et al., 2024; Fu et al., 2025; Lee et al., 2025) using computer-aided virtual screening and other techniques.

However, the umami intensities of peptides are predominantly governed by the peptide chain length, specific amino acid residue composition and sequential arrangement, as well as three-dimensional conformational features (Yang et al., 2024). More specifically, umami peptides elicit their characteristic flavor profile through specific molecular interactions with umami receptors (T1R1/T1R3 receptor) which serves as the primary mediators of umami taste transduction in the gustatory system (Chang et al., 2024; Song, Wang et al., 2025). Although acidic amino acid residues predominantly characterize most umami peptides, the structural conformation of their interaction with umami receptors can be significantly influenced by variations in specific amino acid residues within these peptides (Chang et al., 2024; Song, Zhao, et al., 2025). The binding energies of seven peptides with T1R1/T1R3 receptor ranged from −8.3 to −5.8 kcal/mol with various binding sites (Yu et al., 2024). Chen et al. (2025) identified four critical amino acid residues (Residues of Glu301, Ser217, Asp218, and Arg277) that played essential roles in mediating the interaction between umami peptides and T1R1/T1R3 receptor. Contrary to previous findings, peptides of WGSEPIRIQ and TERGYSF exhibited strong binding affinity to T1R1/T1R3 receptor, as evidenced by their remarkably low docking energies (Lee et al., 2025). Lee et al. (2025) also identified critical hydrogen bonds interacted with specific residues of Ser48, Gly49, and Gln278 in T1R1 subunit, along with residues of Ser67, Asn68, and Arg247 in T1R3 subunit. Consequently, given the structural heterogeneity of peptides and their diverse binding mechanisms with taste receptors, molecular docking emerges as a powerful computational approach to elucidate these complex molecular interactions.

Meretrix lyrata, a highly valued edible shellfish species, is characterized by high protein and low fat contents, rendering it an exceptional source for extracting umami peptides (Hossain et al., 2023; Kong et al., 2023). In our previous study, the proteins of *M. lyrata* can be comprehensively hydrolyzed by protamex, thereby producing the hydrolysate with strong umami and salty tastes (Song, Zhao et al., 2025). Subsequently, a total of 224 umami peptides were screened from *M. lyrata* hydrolysates according to peptidomics and molecular docking. The interactions between umami peptides and the T1R1/T1R3 receptor were systematically summarized, aiming to reveal structure-taste relationships underlying umami taste perception. These findings advance our understanding of marine-derived umami peptides and support their potential application as MSG alternatives in reduced-sodium food products.

2. Materials and methods

2.1. Materials and chemical reagents

Fresh *M. lyrata* was procured from a local aquatic market in Zhanjiang, Guangdong Province, China. After meticulous cleaning and shell removal, *M. lyrata* meat was carefully packaged and subsequently stored at −20 °C in a refrigerator. Protamex (120 U/mg) was obtained from Yuanye Bio-Technology Co., Ltd. (Shanghai, China). T1R3 receptor (BD-PT4502, 93 kDa) and phosphate buffer solution (PBS) were purchased from Biodragon Co., Ltd. (Beijing, China). All compounds and solvents used for sensory purposes were of food-grade quality, whereas the remaining chemical reagents were of analytical grade and sourced from the Chemical Reagent Factory in Guangzhou, China.

2.2. Preparation of protein hydrolysates abundant in umami peptides

M. lyrata hydrolysates abundant in umami peptides were prepared adopting pre-optimized enzymatic hydrolysis conditions (Song, Zhao et al., 2025). In detail, *M. lyrata* meat was finely minced and combined with deionized water at a mass-to-volume ratio of 1:3. The resulting mixture was homogenized at a speed of 10,000 rpm for a duration of 5 min, followed by pH value adjustment to 7.0 by 6.0 M and 0.1 M NaOH. Subsequently, the above samples were subjected to hydrolysis (Protamex-to-protein ratio = 5000 U/g, temperature = 47.8 °C, time = 4.3 h) under optimized conditions to maximize umami peptide yield. Upon completion of the enzymatic hydrolysis, the enzymatic reaction was terminated by heat inactivation in boiling water for 15 min. Following centrifugation (Sorvall LYNX 6000, Thermo Fisher Scientific, USA) at 8000 g for 20 min, the enzymatic hydrolysate was kept at −20 °C for subsequent analysis.

2.3. Peptide sequence analysis by nano LC-MS/MS

The peptide sequence of enzymatic hydrolysate was analyzed following a refined version of the method (Liang et al., 2025). Specifically, enzymatic hydrolysate was initially subjected to ultrafiltration to obtain separate components with a molecular weight less than 3000 Da. The collected fractions were subsequently reduced with iodoacetamide and alkylated with dithiothreitol, followed by desalination using a self-packed desalting column. After these treatments, the sample was then loaded onto a liquid chromatography (LC) column (100 μm i.d. × 180 mm, packing: Reprosil-Pur 120 C18-AQ, 3.0 μm, Thermo Fisher Scientific, USA) (Liang et al., 2025). The mobile phase elution procedure was delivered at a constant flow rate of 600 nL/min with mobile phases A (0.1% formic acid) and B (0.1% formic acid-80% acetonitrile) (0-2 min, linear gradient of liquid B from 4.0 to 8.0%; 2-35 min, linear gradient of liquid B from 8.0 to 28.0%; 35-55 min, linear gradient of liquid B from 28.0 to 40.0%; 55-56 min, linear gradient of liquid B from 40.0 to 95.0%; 56-66 min, linear gradient of liquid B was maintained at 40.0 to 95.0%).

Mass spectrometry conditions: Primary mass spectrometry, resolution: 70000, AGCtarget: 3e6, MaxinumIT: 100 ms, scanning range: 300–1800 m/z; secondary mass spectrometry, resolution: 17500, AGC-target: 1e5, MaximumIT: 50 ms.

2.4. Identification of the peptide sequences

The peptide sequences were identified with minor modifications to established the method (Liang et al., 2025). In the process, the sample was initially collected by LC-MS/MS to generate a raw file of mass spectrometry, which could obtain the peptide sequence and total ion

flow chromatogram. Subsequently, raw mass spectrometry data were analyzed using PEAKS Studio10.6 (Bioinformatics Solutions Inc., Canada), with parameters configured as follows: Fixed modification: Carbamidomethyl (C); variable modification: Oxidation (M), acetyl (N-term); enzyme: No specificity; search database: Uniport Protein (https://www.uniprot.org/) (SequenceVersion 1.0; Downloaded on January 2024); PDR value: 1.0; maximum missed cleavages: 3; peptide mass tolerance: 20 ppm; fragment mass tolerance: 0.02 Da.

2.5. Screening and characterization of umami peptides

The screening and characterization of candidate umami peptides were performed through the taste peptide database (BIOPEP-UWM) combining molecular docking (AutoDockTools-1.5.6). Initial screening focused on umami-specific characteristics, including the identification of key umami-related amino acid residues/segments. Additionally, comprehensive bioinformatic analysis was subsequently conducted to evaluate umami peptide properties, including iso-electric points and net charge content (Analyzed using PepDraw), along with stability parameters (Analyzed using Protparam) such as instability index, aliphatic index, grand average of hydropathicity (GRAVY), and hydrophobicity (Analyzed using PepDraw) (Liang et al., 2025). Moreover, structural predictions were generated using AlphaFold2 (Google DeepMind Inc., USA), with the most reliable models selected for molecular docking.

2.6. Construction and evaluation of the 3D structure of T1R1/T1R3 receptor

Primary sequences of T1R1 subunit (UniProt accession: Q7RTX1) and T1R3 subunit (UniProt accession: Q7RTX0) were sourced from the NCBI protein database. Subsequently, three-dimensional structural models of the T1R1/T1R3 receptor were constructed through homology modelling serving the metabotropic glutamate receptor (PDB ID: 1EWK) as the template, with model construction performed independently in Discovery Studio (Fu et al., 2025) and Swiss-Model (Han et al., 2024). Model quality was rigorously assessed through Ramachandran plot (PROCHECK) and comprehensive validation using the SAVES server (https://saves.mbi.ucla.edu/) (Zhang, He, Liang, Sun, & Zhang, 2024). Following selection of the optimal structural model for molecular docking, detailed characterization was performed, including analysis of amino acid residue composition (Analyzed using Expasy). Additionally, transmembrane domain and N-terminal orientation were predicted using TMHMM-2.0 (https://www.cbs.dtu.dk/services/TMHMM/).

2.7. Molecular docking between umami peptides and T1R1/T1R3 receptor

Molecular docking was used to predict the binding modes and energies using AutoDock Vina (Version 1.5.6) (Lee et al., 2025; Liang et al., 2025) according to the predicted structures of umami peptides and T1R1/T3 receptor independently obtained in sections 2.5 and 2.6. Specifically, the docking mode involved a semi-flexible docking between the umami peptides and T1R1/T1R3 receptor, which was pre-processed by removing small ligands and solvent molecules, followed by hydrogen atom addition using force field parameters. Subsequently, a grid box with dimensions of 150 × 150 × 150 Å and an interval of 0.375 Å was established for docking calculations. After the above preparations, each umami peptide was subjected to ten independent docking simulations with T1R1/T1R3 receptor with the exhaustiveness value set to 10. The most stable binding conformation was identified as the binding conformation of ligand-receptor (Umami peptide-T1R1/T1R3 receptor) exhibiting the lowest docking energy, and the binding results were visualized using PyMol (Schrödinger, LLC., New York, NY, USA) and Discovery Studio (DS) 2019 (BIOVIA Inc., USA). Furthermore, DS was also employed to investigate the interaction forces between ligands and residues at T1R1/T1R3 receptor binding sites.

2.8. Verification of the taste mechanism of umami peptides

2.8.1. Microstructure determination

Following the virtual screening results, selected representative umami peptides were chemically synthesized by China Peptides Qyaobio Co., Ltd. (Shanghai, China) with the purity grade exceeding 95 %. Atomic force microscopy (AFM, Dimension Edge, Bruker, USA) was employed to characterize microstructural modifications of T1R3 receptors induced by MSG and umami peptides (Sun et al., 2025). Freshly exfoliated mica sheet was first functionalized with 20.0 μL of T1R3 receptor solution (5.0 μg/mL in PBS) for 20 min adsorption. Subsequently, 20.0 μL MSG and umami peptide solutions (10.0 μg/mL in PBS) were deposited and allowed to incubate for 20 min. Following dehydration at 30 °C for 2 h, samples were imaged using an AFM system operating in tapping mode (25 °C, 1.0 Hz scan rate). All images were processed by NanoScope Analysis software (Waters Asia Limited, Shanghai, China) (Sun et al., 2025).

2.8.2. Determination of interaction parameters between umami peptides and T1R3 receptor

Thermodynamic characterization of T1R3 receptor-umami peptide interactions was performed using isothermal titration calorimetry (HS-T220 ITC, HONSEN Ltd., Changsha, China) (Li et al., 2024). The interactions were conducted by titrating 0.1000 mM peptide solution into 0.0570 mM T1R3 receptor (both dissolved in PBS buffer) at 25 °C. The titration measurements consisted of twenty-successive 5.0 μL injections at 2.0 μL/s injection speed, with 240 s intervals between injections. The HS-T220 analyzer software (HONSEN Ltd., Changsha, China) derived key thermodynamic parameters including dissociation constant (*Ka*), binding affinity constants (*Kd*), junction site (n), Gibbs free energy (*ΔG*, kJ/mol), reaction heat (*ΔQ*, μW), enthalpy (*ΔH*, kJ/mol), and entropy (*ΔS*, kJ/mol). The key Van't Hoff equation was calculated by formulas following:

$$\mathrm{lnKa} = \ln\frac{1}{\mathrm{Kd}} = -\frac{\Delta \mathrm{H}}{\mathrm{RT}} + \frac{\Delta \mathrm{S}}{\mathrm{R}} \tag{1}$$

$$\triangle \mathrm{G} = -\mathrm{RTlnKa} \tag{2}$$

$$-\mathrm{T}\triangle \mathrm{S} = \triangle \mathrm{G} - \triangle \mathrm{H} \tag{3}$$

In the Equations, *R* denotes the universal gas constant (8.314 J/mol·K) and *T* indicates the Kelvin temperature.

2.8.3. Determination of the umami taste of umami peptides

The umami intensity of the umami peptides was conducted with minor modifications (Song et al., 2024). The peptide solutions were prepared by dissolving the synthesized peptides in deionized water to gradient concentrations (0.0625, 0.125, 0.25, 0.50 and 1.00 mg/mL), followed by filtration through dual-layer filter paper. Subsequently, the umami intensity of the umami peptides was determined using an electronic tongue system (SA402B, Insent Ltd., Japan) equipped with cross-selective taste oscillation (CTO) sensor and autonomous array electrode (AAE) sensor. MSG solution at equivalent concentration was used as the reference standard.

2.8.4. Sensory evaluation of the umami taste of umami peptides

Sensory evaluation of umami peptides was conducted using Quantitative Descriptive Analysis (QDA) following the method described by Yang et al. (2022). The ten-point scoring system was designed as follows: Very weak (0–2 scores), weak (2–4 scores), medium (4–6 scores), strong (6–8 scores), and very strong (8–10 scores). This scoring system provided a quantitative framework for umami intensity assessment. The umami intensity of a 0.01 mg/mL MSG standard solution was scored as "0 score", whereas that of a 1.00 mg/mL MSG standard solution was scored as "10 scores". For evaluation, 20.0 mL of umami peptide solutions were transferred into clean, transparent cups and labeled with

randomized three-digit codes. After equilibrating at room temperature (25 °C) for 30 min, the taste of the umami peptides was assessed by 20 trained food professionals (Aged between 20 and 30), experienced in umami peptide assessment. Trained panelists independently evaluated each sample and rated the perceived umami intensity using the established scale. All sensory evaluations were conducted under the same environmental conditions to minimize external variability.

2.9. Statistical analysis

Each experiment was independently replicated three or more times with a variety of samples. Statistical analysis, including ANOVA and Duncan's Multiple Range tests, was carried out using SPSS software (version 19.0; SPSS Inc., Chicago, IL, USA). Data were expressed as mean ± standard deviation (SD).

3. Results and discussion

3.1. Bioinformatics analysis of umami peptides

Based on peptidomics and molecular docking, a total of 224 umami peptides were screened from *M. lyrata* hydrolysates. The chain lengths of these peptides ranged from 4 to 11 amino acid residues (AARs), a chain length range ideal for umami peptides. To systematically investigate their taste characteristics, 224 varieties of umami peptides were divided into three groups according to their chain lengths: Group I (72 umami peptides with chain lengths from 4 to 7 AARs), Group II (73 umami peptides with chain lengths from 8 to 9 AARs), and Group III (79 umami peptides with chain lengths from 10 to 11 AARs). Subsequently, these groups were subjected to comprehensive bioinformatics analysis, as presented in Fig. 1. Specifically, most umami peptides displayed stable structures that were difficult to break down due to their instability index below 40 [Fig. 1(A)]. With increasing peptide chain length, the isoelectric points of umami peptides trended toward an alkaline direction [Fig. 1(B)], consistent with the observed variations in net charge contents (pH7.0) of the peptides [Fig. 1(C)]. Furthermore, the lowest isoelectric point and the highest net charge contents were found in umami peptides with the chain length of 4–7 AARs, indicating that short-chain umami peptides were associated with more pronounced umami taste. In contrast to HEAEEVHEE and DTEEVEHGEE, TPIPDLP, a low-molecular weight peptide isolated and purified from Yanjin black bone chicken, was identified as the most potent umami peptide (Yang et al., 2025). Six umami peptides (LPTPR, WPDA, ADGDF, WGDE, WDDM, and ALMM) were also identified from low-salt air-dried chicken, with umami thresholds ranging from 0.45 to 1.68 mmol/L, and LPTPR displayed the most prominent umami taste (Yu et al., 2024).

Besides, the aliphatic index and GRAVY of umami peptides could serve as indicators of side chain hydrophobicity [Fig. 1(D–E)], and both indicators exhibited a parallel trend due to their insensitivity to peptide chain length (Liang et al., 2025). However, the hydrophobicity of umami peptides rose notably with extended peptide chain lengths, but their values were primarily concentrated below 20 kcal/mol [Fig. 1(F)]. This suggested that the umami peptides were highly hydrophilic and exhibited excellent solubility in aqueous solutions [Fig. 1(F)]. A series of umami peptides were identified to contain abundant acidic amino acid residues, which served as typical polar residues that could contribute to strong hydrophilicity (Chang et al., 2024; Song, Wang et al., 2025; Yang et al., 2024). As a result, in contrast to long-chain umami peptides, short-chain umami peptides tend to show strong umami taste due to their iso-electric points and high net charge contents. To further elucidate the role of these 224 umami peptides in taste perception, it was required to conduct more in-depth analysis of their taste effects and the mechanisms underlying their taste characteristics.

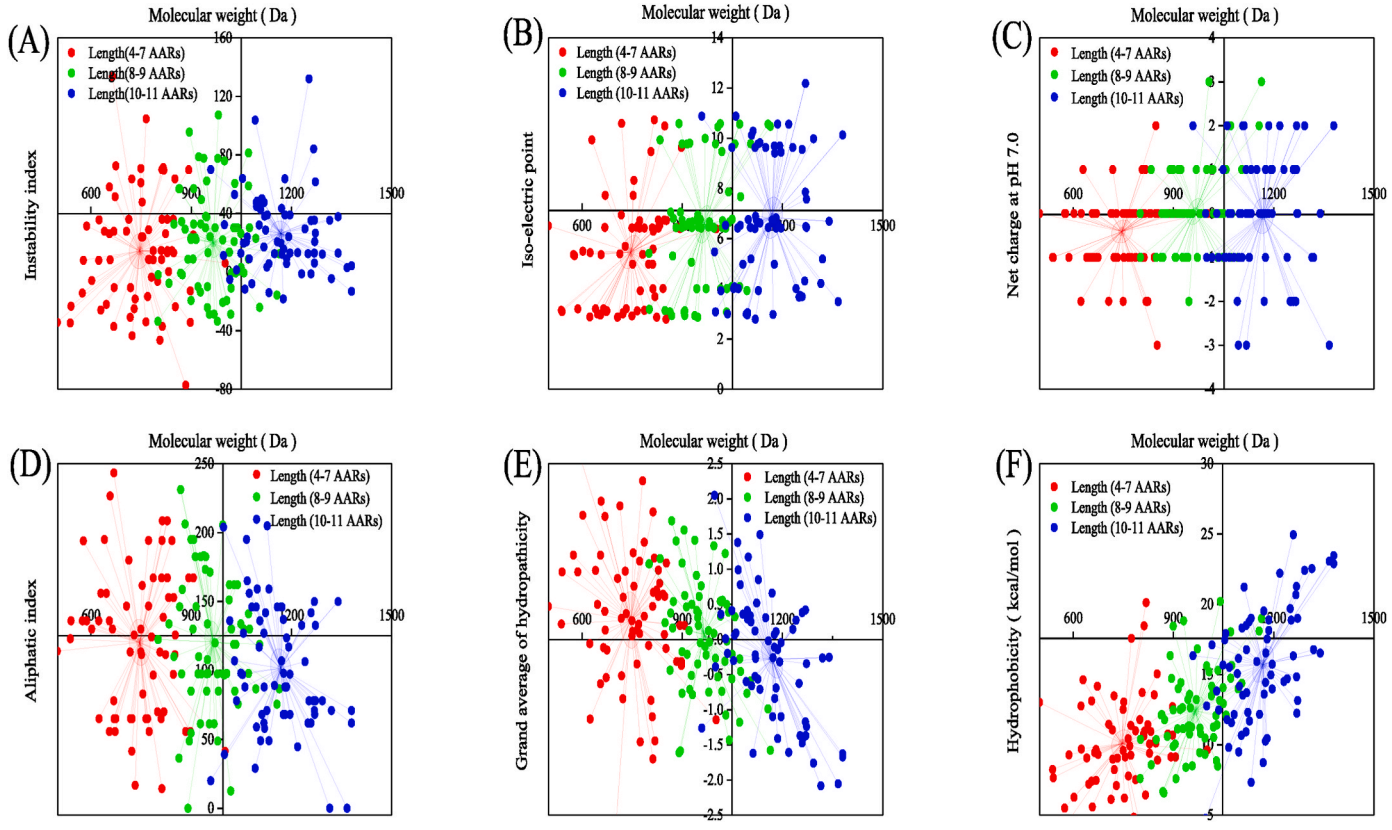

Fig. 1. Biological information analysis of umami peptides derived from the protein hydrolysate of *Meretrix lyrata*. (A) Instability index, (B) iso-electric point, (C) net charge at pH 7.0, (D) aliphatic index, (E) grand average of hydropathicity (GRAVY), (F) hydrophobicity.

3.2. Analysis of structural characteristics of umami peptides

As shown in Fig. 2(A–C) and S1, the umami flavor of umami peptides was attributed to acidic amino acid residues and related fragments in their structure. Besides, the structure of umami peptides featured hydrophobic amino acid residues in addition to a high number of acidic amino acid residues, providing multiple potential docking sites for interaction with umami receptors [Fig. 2(D)]. In addition, umami peptides with 4–7 AARs displayed an average molecular weight of 750 Da, those with 8–9 AARs averaged 1000 Da, and those with 10–11 AARs averaged 1200 Da, with all mass-charge ratios distributed around 500 [Fig. 2(E–F)]. The results indicated that the charge of umami peptides increased with the increase of their molecular weight. Identified umami peptides, characterized by their low molecular weight (500–1000 Da) and short amino acid sequences, exhibit enhanced umami taste perception due to their optimal size for taste receptor interaction (Song, Zhao et al., 2025; Yu et al., 2024). Moreover, the umami peptides contained nearly equal proportions of hydrophilic and hydrophobic amino

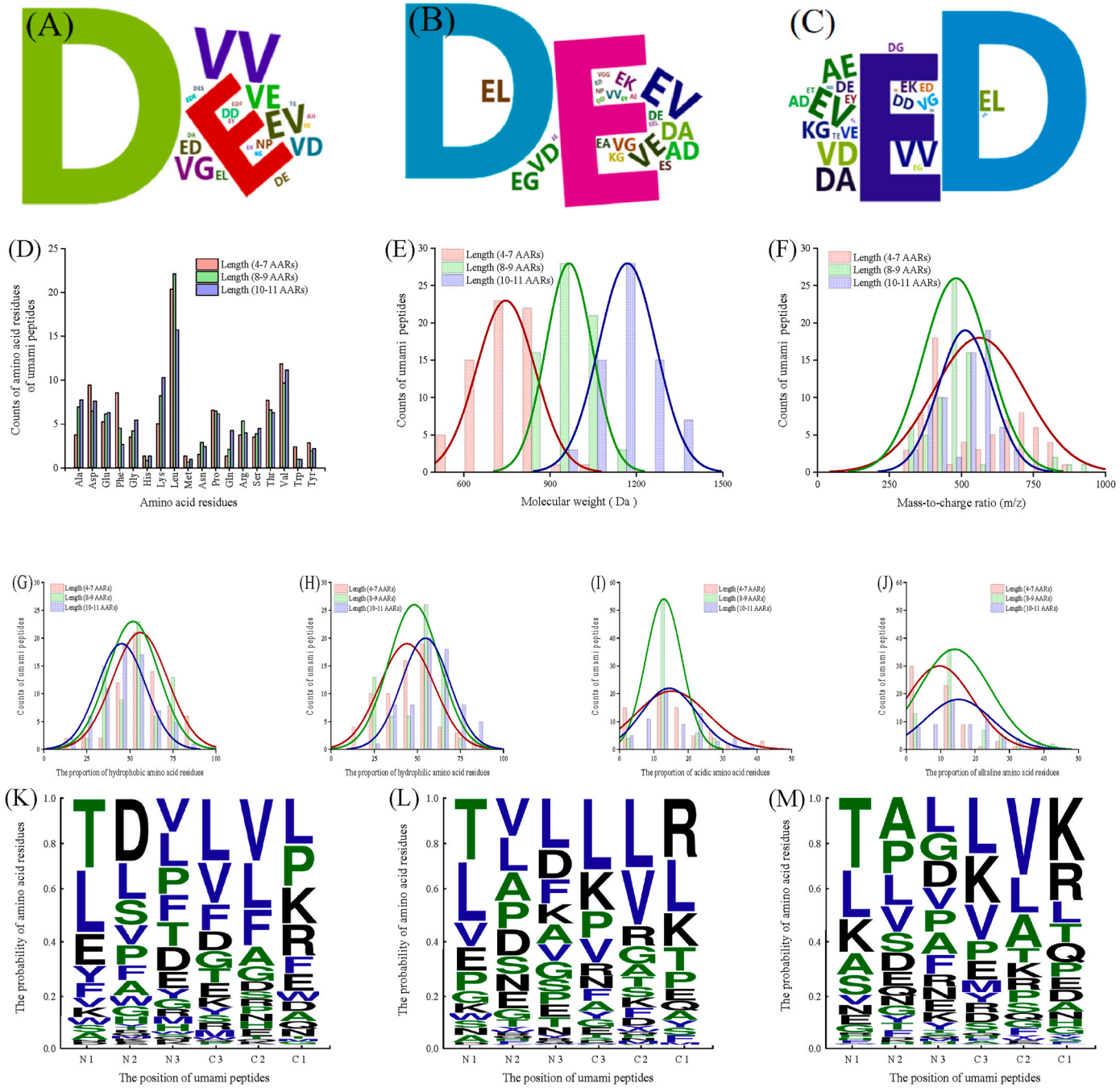

Fig. 2. The physicochemical characteristics of umami peptides derived from the protein hydrolysate of *Meretrix lyrata*. (A) Umami fragments/amino acid residues of umami peptides with 4–7 amino acid residues, (B) umami fragments/amino acid residues of umami peptides with 8–9 amino acid residues, (C) umami fragments/amino acid residues of umami peptides with 10–11 amino acid residues, (D) composition and proportion of amino acid residues, (E) molecular-weight distributions, (F) distributions of mass-to-charge ratio (m/z), (G) distributions of hydrophobic amino acid residue proportion, (H) distributions of hydrophilic amino acid residue proportion, (I) distributions of acidic amino acid residue proportion, (J) distributions of alkaline amino acid residue proportion, (K) the motif's logo of umami peptides with 4–7 amino acid residues, (L) the motif's logo of umami peptides with 8–9 amino acid residues, (M) the motif's logo of umami peptides with 10–11 amino acid residues.

acid residues, which together accounted for approximately 50 % of the total residues, with acidic and alkaline amino acid residues reaching up to 10 % [Fig. 2(G–J)]. Specifically, these polar amino acid residues could create abundant docking sites for umami peptides, in agreement with previous studies which reported umami peptides interacting with umami receptor *via* ionic and hydrogen bonds (Amin et al., 2020; Chang et al., 2024; Yang et al., 2025). Cui et al. (2024) also highlighted that the carboxyl (-COOH) and amino (-NH_2) groups of acidic and basic amino acids within the umami peptide could form hydrogen bonds with polar charged amino acid residues located on umami receptors.

As shown in Fig. 2(K–M), the characteristic N- and C-terminal amino acid residues of umami peptides were predominantly composed of polar and hydrophobic amino acid residues, aligning with the findings presented in Fig. 2(A–D). Similar findings were also reported in a study which reported that polar and hydrophobic amino acid residues were cross arranged in active peptides to stabilize their conformation (Liang et al., 2025). Moreover, hydrophilic amino acid residues were primarily located at the N- and C-terminus, whereas hydrophobic amino acid residues were concentrated in the central region of umami peptides. Consequently, polar amino acid residues could provide an abundance of cations, anions, and strongly electronegative atoms, allowing umami peptides to interact with umami receptors *via* ionic and hydrogen bonds (Jia et al., 2024; Zhang, Tu, Wen, Wang, & Hu, 2024). Besides, hydrophobic amino acid residues could form hydrophobic bonds to promote the interaction between umami peptides and their receptors (Cao et al., 2023; Jia et al., 2024; Zhang, Tu, Wen, Wang, & Hu, 2024). Similar to polar amino acid residues, hydrophobic amino acid residues also functioned as hydrogen donors, urging tightly to interact with the receptors *via* hydrogen bonds (Cao et al., 2023; Jia et al., 2024; Zhang, Tu, Wen, Wang, & Hu, 2024).

Regarding the structural features of umami peptides, negative charged functional groups (-COO^-) acted as taste-determining groups, while hydrophilic functional groups (-OH and α-L-NH_2) acted as taste-promoting groups (Lindemann, 2001; Roper & Chaudhari, 2017; Yan & Tong, 2022). When these functional groups bound to umami receptors *via* chemical bonds, the taste receptors were activated and transformed their structure into an active one (Lindemann, 2001; Roper & Chaudhari, 2017; Yan & Tong, 2022). As a result, polar and hydrophobic amino acid residues were vital binding sites for umami peptides, mediating their interactions with umami receptors *via* chemical bonds. Specifically, umami receptors could quickly identify and combine with the peptides containing polar and hydrophobic amino acid residues. Yu et al. (2024) emphasized that the essential amino acid residues of Tyr, Ser, Asn, His, and Glu in the umami taste receptors T1R1/T1R3 were identified as critical for peptide binding. Therefore, umami peptides were high in these residues which could provide numerous binding sites for umami peptides, with the interactions potentially including ionic, hydrogen, and hydrophobic bonds.

3.3. Structural prediction and evaluation analysis of T1R1/T1R3 receptor

As shown in Fig. 3 and S1, three variants of T1R1/T1R3 receptor were constructed based on two AI de novo folding methods, all sharing highly similar three-dimensional structures. Among these, the blue variant exhibited a structure more closely resembling the template (1EWK) than other T1R1/T1R3 receptors [Fig. 3(A–B)], aligning with the structures reported by Lee et al. (2025) and Zhang, Tu, Wen, Wang, & Hu. (2024). In addition, while merely 0.8 % of residues were positioned in disallowed regions, the blue one comprised 99.2 % (>90 %) of residues in allowed regions, with 89.1 % in the most favored region and 10.1 % in additional and generously allowed regions, demonstrated the rationality and reliability of the T1R1/T1R3 receptor model [Fig. 3 (C–D)]. Consequently, the blue T1R1/T1R3 model was validated as dependable and well-suited for application as an umami receptor in advanced molecular docking studies.

As depicted in Fig. 3(E–G), the T1R1/T1R3 receptor exhibited a generally equal proportion of hydrophobic and hydrophilic amino acid residues, with each type accounting for half of the total residues, which contributed to a balanced surface potential distribution. Hence, this stability of the T1R1/T1R3 receptor model provided additional evidence for its rationality and reliability. Additionally, the receptor was predominantly constructed from Leu, Ala, Val, Ser, Arg, and Gly residues, which matched the composition of umami peptides characterized by high levels of polar and hydrophobic amino acid residues. Therefore, hydrophobic and ionic bonds likely played key roles in bridging umami peptides to their receptors. Subsequently, these residues could also function as hydrogen donors, facilitating hydrogen bond formation for the interactions (Cao et al., 2023; Jia et al., 2024; Zhang, Tu, Wen, Wang, & Hu, 2024). As a result, the formation of these chemical bonds drove the formation of a receptor-ligand binding conformation between umami peptides and the T1R1/T1R3 receptor with the lowest docking energy. Moreover, T1R1/T1R3 receptor was characterized by its heterodimeric structure, consisting of two distinct subunits (T1R1 and T1R3 subunits) (Cao et al., 2023; Yao et al., 2024). The T1R1/T1R3 receptor was composed of thirteen transmembrane domains, including seven from the T1R1 subunit and six from the T1R3 subunit, which collectively formed a functional receptor complex (Cao et al., 2023; Yao et al., 2024; Yu et al., 2025). Besides, In addition, T1R1/T1R3 receptor functioned as a canonical transmembrane protein, with its N-terminus located outside the cell membrane, and the beginning and ending positions of the transmembrane domains were shown in Fig. 3(H–I) and Tables S1–S2.

3.4. Analysis of binding energy and visualization of molecular docking

The interaction mechanism between umami peptides and T1R1/T1R3 receptor was elucidated by simulating their spatial conformation and energy complementarity using AutoDock Vina, employing a semi-flexible docking approach (Liang et al., 2025; Yu et al., 2025). A total of 224 umami peptides were screened and docked to T1R1/T1R3 receptor, with their binding energy averaging −7.4 kcal/mol [Fig. 4 (A–B)]. Owing to their analogous amino acid residue composition and sequence, umami peptides tended to share similar structural conformations, causing their binding energies to remain unaffected by variations in peptide chain lengths (Cao et al., 2023; Jia et al., 2024).

In addition, several typical binding conformations of the receptor-ligand complexes between MSG/umami peptides and T1R1/T1R3 receptor were visualized and analyzed, as depicted in Fig. 4(C–F). Hydrogen and ionic bonds were vital forces driving the binding interaction between MSG and T1R1/T1R3 receptor. However, owing to their multiple amino acid composition, umami peptides exhibit greater structural complexity than MSG. The binding mechanisms between umami peptides and T1R1/T1R3 receptor were mediated by ionic, hydrophobic, and hydrogen bonds, with hydrophobic and hydrogen bonds being the primary driving forces. The result aligned with the analysis presented in Figs. 2 and 3. In addition, MSG showed preferential affinity for the binding pocket of T1R1 subunit, whereas umami peptides exhibited more extensive interactions with both subunits. Upon recognition of the umami peptide by T1R1 subunit, a conformational change in T1R3 subunit occurs for embodying the peptide, further expanding its binding cavity and facilitating subsequent ligand binding (Yang et al., 2025). In particular, hydrogen bonds exhibited a uniform distribution during the molecular docking of umami peptides with T1R1/T1R3 receptor, and those with shorter bond lengths were shown to directly enhance the stability of the receptor-peptide binding conformation (Cao et al., 2023; Jia et al., 2024; Zhang, Tu, Wen, Wang, & Hu, 2024). Most importantly, the stability of the receptor-peptide binding conformation was largely determined by the structure and physicochemical properties of umami peptides, resulting in variations which were primarily manifested in chemical bonds and binding sites of the conformations (Jia et al., 2024; Yu et al., 2024). Accordingly, extensive molecular docking of umami peptides to T1R1/T1R3 receptor was performed, followed by

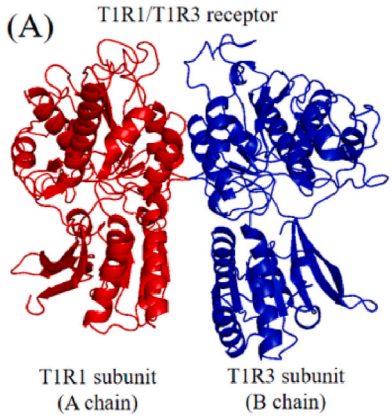

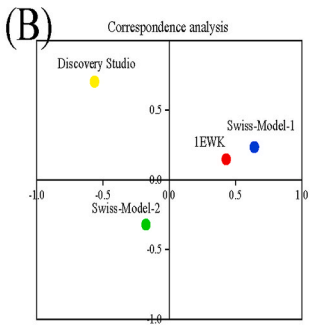

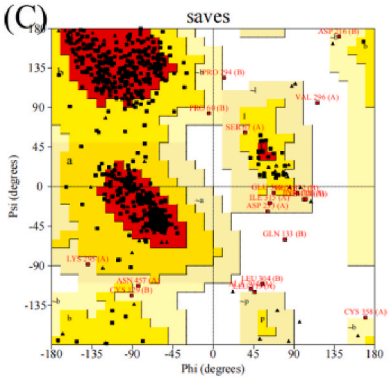

(D)

Plot statistics

Residues in most favoured regions [A,B,L]	704	89.1%
Residues in additional allowed regions [a,b,l,p]	69	8.7%
Residues in generously allowed regions [~a,~b,~l,~p]	11	1.4%
Residues in disallowed regions	6	0.8%
Number of non-glycine and non-proline residues	790	100.0%
Number of end-residues (excl. Gly and Pro)	4	
Number of glycine residues (shown as triangles)	65	
Number of proline residues	44	
Total number of residues	903	

Based on an analysis of 118 structures of resolution of at least 2.0 Angstroms and R-factor no greater than 20%, a good quality model would be expected to have over 90% in the most favoured regions.

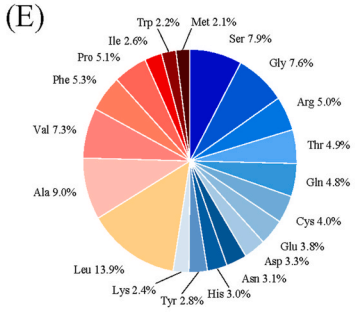

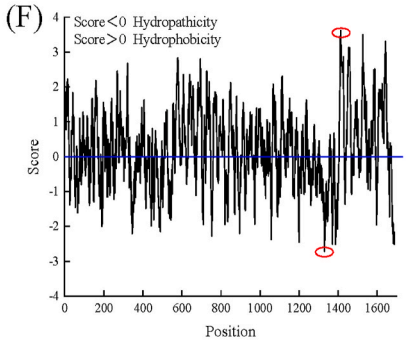

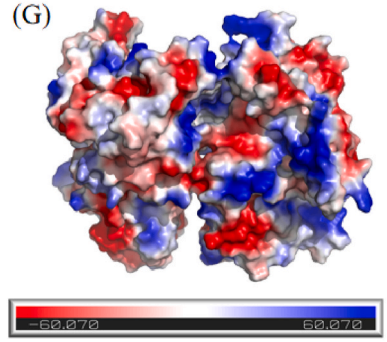

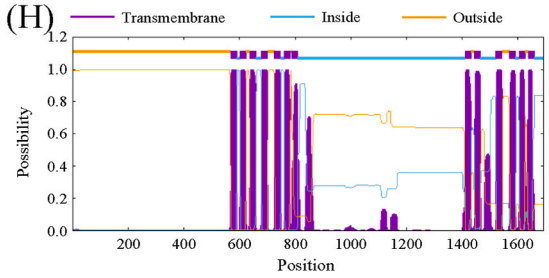

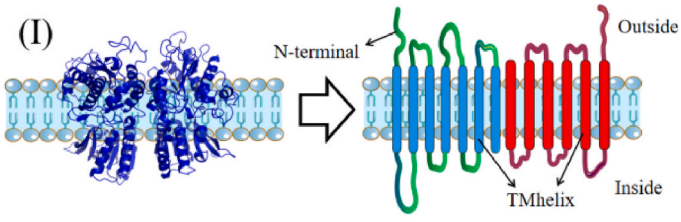

Fig. 3. Constructed the 3D structure of T1R1/T1R3 receptor using Swiss-Model software and evaluated it by Ramachandran plot. (A) The 3D structure of T1R1/T1R3 receptor, (B) correlation analysis of T1R1/T1R3 receptor and its template (1EWK), (C) Ramachandran Plot, (D) plot statistics, (E) composition and proportion of amino acid residues, (F) hydropathicity score of amino acid residues, (G) surface potential distribution, (H) distribution of transmembrane structures, (I) transmembrane structure.

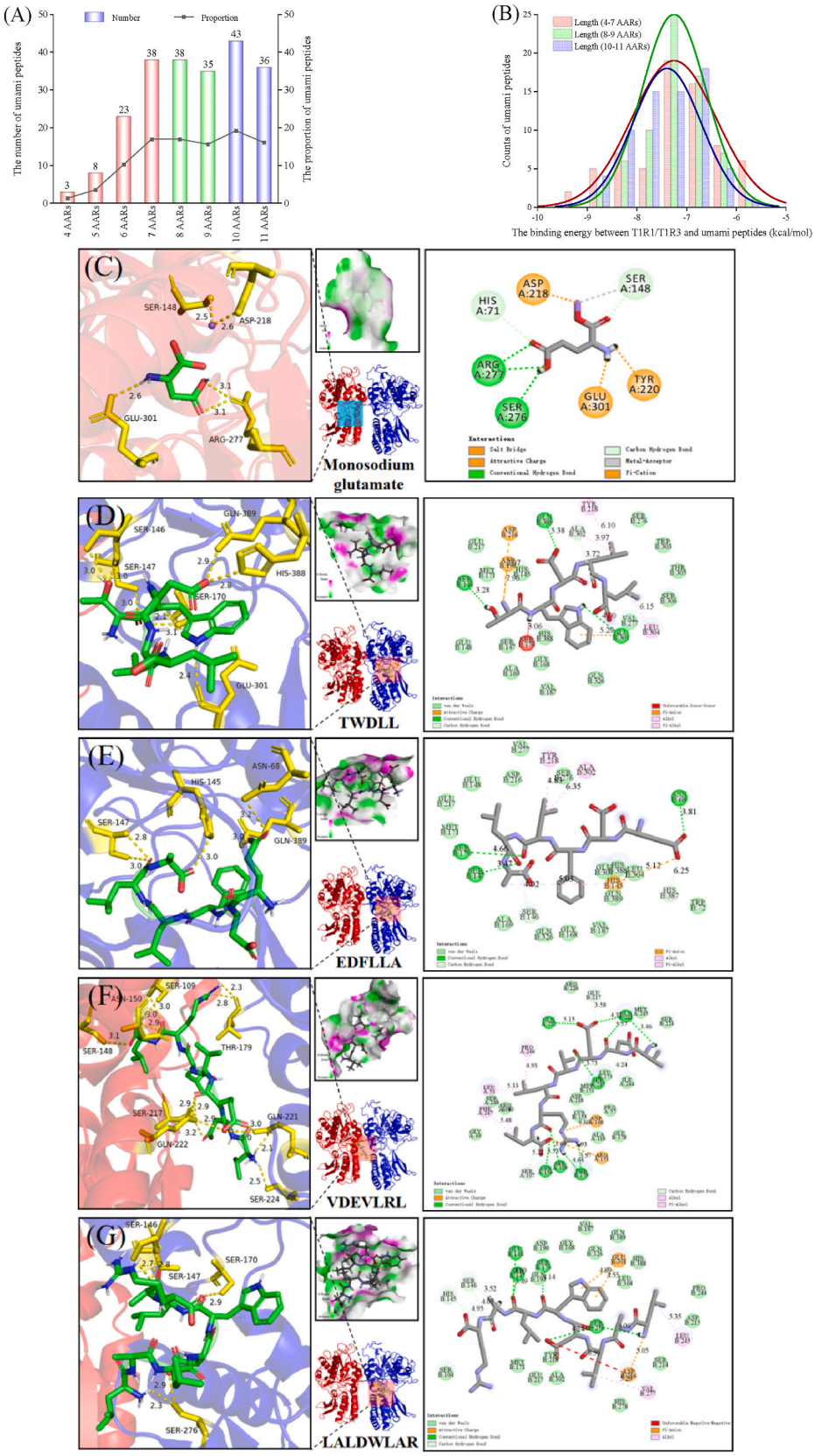

Fig. 4. The distributions of binding energy between umami peptides and T1R1/T1R3 receptor, and the molecular docking visualization of them. (A) Classification and number of umami peptides, (B) distributions of binding energy, (C) visualization of monosodium glutamate, (D) visualization of TWDLL, (E) visualization of EDFLLA, (F) visualization of VDEVLRL, (G) visualization of LALDWLAR.

statistical analysis of the docking data to identify key chemical interactions and binding sites underlying their interactions.

3.5. Characterization of the intramolecular chemical bonds within umami peptides during molecular docking

Under the influence of T1R1/T1R3 receptor, umami peptides might form intramolecular chemical bonds within the peptides, thereby modifying their structure during ligand-receptor interactions. Subsequently, the functional groups that umami peptides bonded to T1R1/T1R3 receptor were disrupted the functional groups involved in binding, which varied the umami peptides and the receptor, thereby directly affecting their interactions (Han et al., 2024; Yao et al., 2024). Hence, a competitive relationship emerged between the chemical bonds formed by the umami peptide alone and those generated by the umami peptide in conjunction with T1R1/T1R3 receptor. Moreover, the intramolecular chemical bonds within the umami peptide were capable of modifying its spatial conformation, increasing its flexibility and facilitating more effective interactions with umami receptors (Han et al., 2024; Yao et al., 2024).

As shown in Fig. 5, the umami peptides formed multiple intramolecular chemical interactions, including ionic, hydrophobic, and hydrogen bonds. Notably, the specific amino acid residues engaged in these interactions remained unaffected by variations in peptide chain length. Moreover, during molecular docking of 224 distinct umami peptides with T1R1/T1R3 receptor, both ionic and hydrophobic bonds demonstrated remarkably uniform distributions, with each bond maintaining an average of one bond per peptide [Fig. 5(A–B)]. In contrast, hydrogen bonds displayed a highly uneven distribution, with their number increasing as peptide chain length increased, averaging five bonds per umami peptide [Fig. 5(C)]. During the formation of ionic bond within umami peptides, residues of hydrophobic and alkaline amino acids primarily supplied cations (H^+ and NH_3^+), whereas acidic amino acids acted as the main contributors of anions ($-COO^-$) [Fig. 5(D)]. In addition, hydrophobic bonds were facilitated by hydrophobic amino acid residues in umami peptides, including residues of Leu, Phe, and Val [Fig. 5(E)]. In contrast to the previous two chemical bonds, a variety of amino acid residues were involved in the formation of hydrogen bonds, including residues of Asp, Glu, Lys, Arg, and Leu [Fig. 5(F)]. Among them, hydrophobic and alkaline amino acid residues were predominantly responsible for supplying hydrogen atoms during hydrogen bond formation within umami peptides, whereas hydrophobic and polar residues acted as the primary sources of oxygen or other electronegative atoms (Nitrogen atom). Consequently, these findings were in agreement with the results depicted in Fig. 2, confirming that umami peptides were abundant in acidic and hydrophobic amino acid residues.

3.6. Analysis of intermolecular chemical bonds and key binding sites between umami peptides and T1R1/T1R3 receptor

As shown in Fig. 6, the interactions between umami peptides and T1R1/T1R3 receptor involved ionic, hydrophobic, and hydrogen bonds, with hydrophobic and hydrogen bonds serving as the key chemical bonds, as evidence by each umami peptide forming both bonds during interactions with the receptor. The formation of these bonds was primarily determined by the physicochemical properties and amino acid residue composition of the peptides during the interactions between umami peptides and T1R1/T1R3 receptor (Cao et al., 2023; Jia et al., 2024; Zhang, Tu, Wen, Wang, & Hu, 2024). Consequently, during the interactions between umami peptides and the receptor, comprehensive analyses of the chemical bonds and their key docking residues were essential to elucidate the molecular mechanism of umami flavor.

As shown in Fig. 6(A–F), the ionic bonds formed in the interactions between umami peptides and T1R1/T1R3 receptor were classified into two types, with each type averaging one bond per peptide. However, these bonds were independent of peptide chain length, aligning with the results depicted in Fig. 2, indicating that umami peptides contained acidic and alkaline amino acid residues, each accounting for 10 % of the

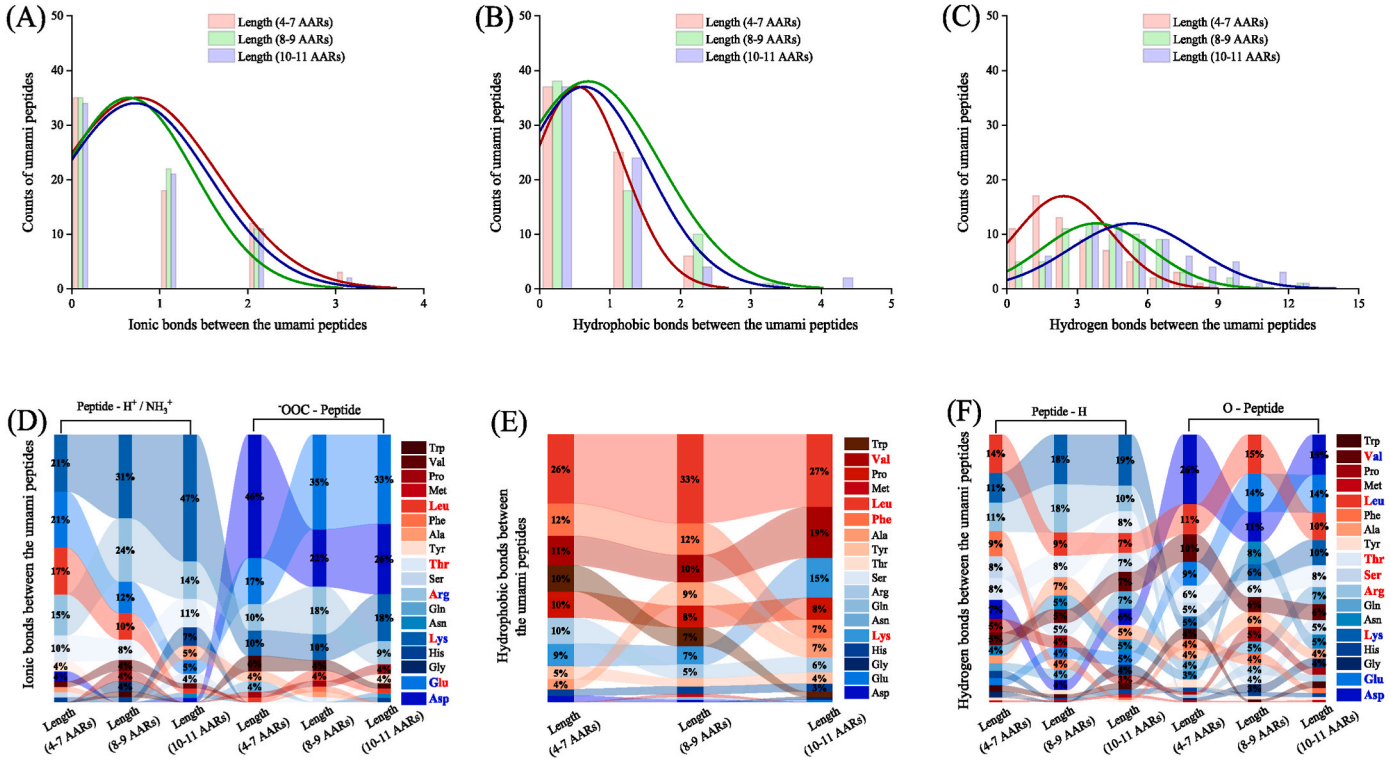

Fig. 5. The internal chemical bonds formed within the umami peptide during molecular docking. (A) Distributions of ionic bonds, (B) distributions of hydrophobic bonds, (C) distributions of hydrogen bonds, (D) amino acid residues forming ionic bonds, (E) amino acid residues forming hydrophobic bonds, (F) amino acid residues forming hydrogen bonds.

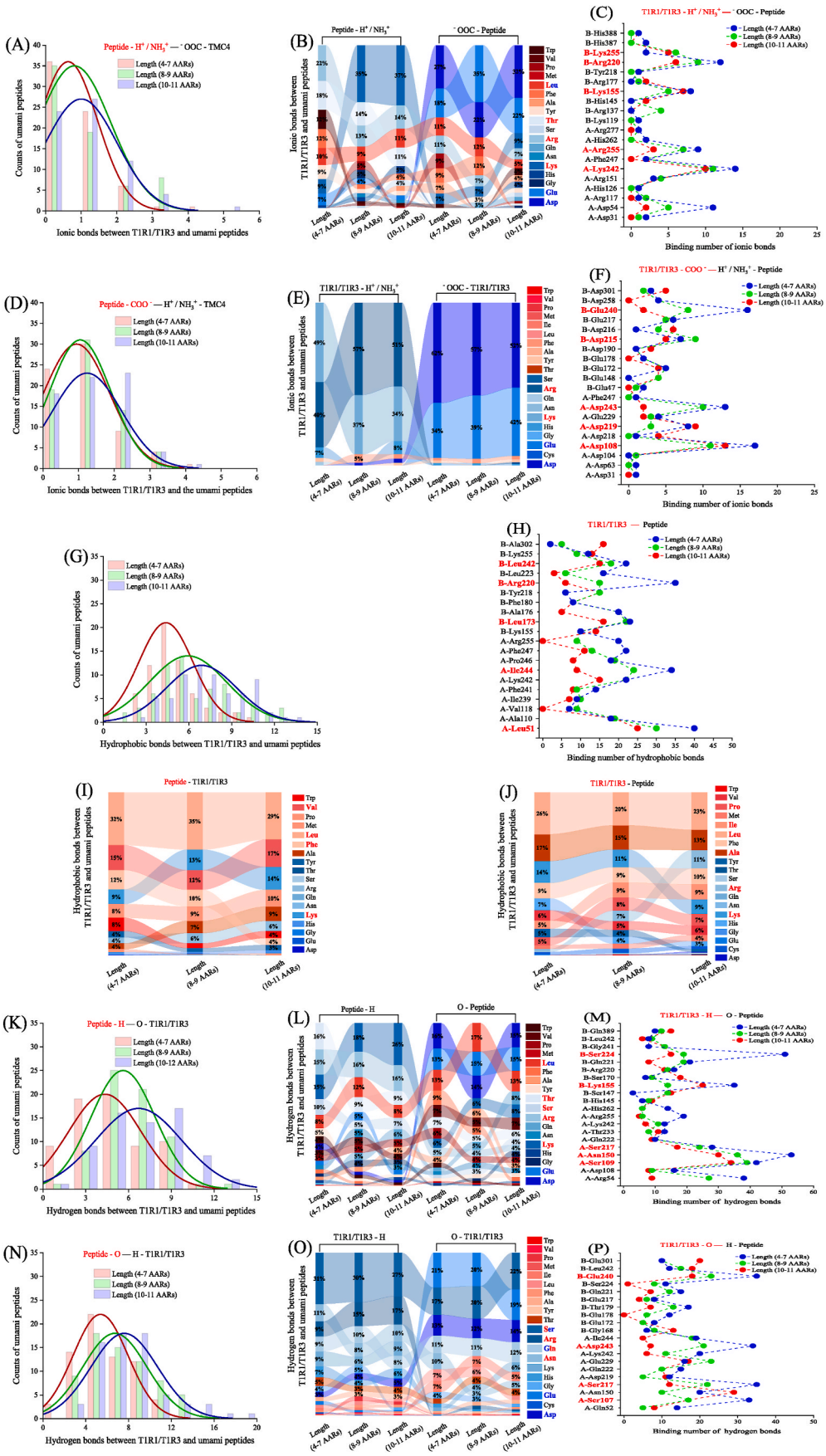

(caption on next page)

Fig. 6. The chemical bonds formed between umami peptides and T1R1/T1R3 receptor. (A) Distributions of ionic bonds (Type I), (B) amino acid residues of umami peptides forming ionic bonds, (C) crucial binding sites of ionic bonds in T1R1/T1R3 receptor (Type I), (D) distributions of ionic bonds (Type II), (E) amino acid residues of T1R1/T1R3 receptor forming ionic bonds, (F) crucial binding sites of ionic bonds in T1R1/T1R3 receptor (Type II), (G) distributions of hydrophobic bonds, (H) crucial binding sites of hydrophobic bonds in T1R1/T1R3 receptor, (I) amino acid residues of umami peptides forming hydrophobic bonds, (J) amino acid residues of T1R1/T1R3 receptor forming hydrophobic bonds, (K) distributions of hydrogen bonds (Type I), (L) amino acid residues of umami peptides forming hydrogen bonds, (M) crucial binding sites of hydrogen bonds in T1R1/T1R3 receptor (Type I), (N) distributions of hydrogen bonds (Type II), (O) amino acid residues of T1R1/T1R3 receptor forming hydrogen bonds, (P) crucial binding sites of hydrogen bonds in T1R1/T1R3 receptor (Type II). Among them, the ionic bond (Peptide - H^+/NH_3^+ — ^-OOC - T1R1/T1R3) was labeled as Type I; the ionic bond (Peptide -COO^- — H^+/NH_3^+ - T1R1/T1R3) was labeled as Type II; the hydrogen bond (Peptide - H — O - T1R1/T1R3) was labeled as Type I; the hydrogen bond (Peptide - O — H - T1R1/T1R3) was labeled as Type II.

total residues. Among them, one type (Type I) of ionic bond was formed between cations (H^+ and NH_3^+) supplied by umami peptides and anions (-COO^-) provided by T1R1/T1R3 receptor. Conversely, anions (-COO^-) from umami peptides interacted with cations (H^+ and NH_3^+) from T1R1/T1R3 receptor to form the second type (Type II) of ionic bond. In the structures of umami peptides or T1R1/T1R3 receptor, the cations were primarily contributed by alkaline amino acid residues, whereas the anions were primarily derived from acidic amino acid residues. Therefore, the vital binding sites responsible for supplying cations to form ionic bonds were residues of Lys242 and Arg255 in T1R1 subunit, along with residues of Lys155, Arg220, and Lys255 in T1R3 subunit. Besides, the vital binding sites supplying anions for ionic bonds were residues of Asp108, Asp219, and Asp243 in T1R1 subunit, as well as residues of Asp215 and Glu240 in T1R3 subunit.

As shown in Fig. 6(G–J), hydrophobic bonds between umami peptides and T1R1/T1R3 receptor displayed a highly uneven distribution, increasing in number as peptide chain length increased, averaging from 4.0 to 7.5 bonds per peptide. Hydrophobic amino acid residues were the primary contributors to hydrophobic bonds during the interactions between umami peptides and T1R1/T1R3 receptor. More specifically, residues of Leu, Phe, Val and Lys within umami peptides were predominantly contributors to hydrophobic bonds, whereas those in T1R1/T1R3 receptor were primarily residues of Ala, Leu, Ile, Pro, and Arg, due to the abundance of these residues in their respective structures. Therefore, the vital binding sites responsible for hydrophobic bonds were residues of Leu51 and Ile244 in T1R1 subunit, along with residues of Leu173, Arg220, and Leu242 in T1R3 subunit.

As shown in Fig. 6(K–P), two kinds of hydrogen bonds also played key roles in promoting the interactions between umami peptides and T1R1/T1R3 receptor, with each type averaging six bonds per peptide. In particular, both bonds became more numerous as the peptide chain lengths grew longer. Comparable to ionic bonds, one type (Type I) of hydrogen bond was formed between hydrogen atoms of umami peptides and oxygen atoms of T1R1/T1R3 receptor. In contrast, the other hydrogen bond (Type II) was formed reversely, involving oxygen atoms from umami peptides and hydrogen atoms from the receptor. More specifically, umami peptides were characterized by diverse amino acid residues which could donate hydrogen atoms for the formation of hydrogen bonds, including alkaline, hydrophilic, and hydrophobic amino acids. Conversely, the predominant amino acid residues contributing oxygen atoms were identified as Asp, Glu, and Leu residues. Due to their similar chemical structures and identical spatial conformations, the umami peptides could recognize and bind to the same specific region of T1R1/T1R3 receptor (Chang et al., 2024; Song, Wang et al., 2025; Yang et al., 2024). As a result, the distribution of hydrogen and oxygen atom-donating residues for hydrogen bonds within T1R1/T1R3 receptor exhibited highly concentrated, with residues of Asn, Gln, Arg, and Ser serving as primary hydrogen atom donors, whereas residues of Asp, Glu, and Gln functioned as the predominant oxygen atom donors. Moreover, Glu is a negatively charged polar amino acid that serves as an excellent hydrogen bond acceptor. Besides, Ser, a hydrophilic amino acid containing polar hydroxyl groups, is typically localized on the surface of globular proteins (Guo, Ren, et al., 2024; Rapino et al., 2021). The umami peptides from chicken soup bound to T1R1/T1R3 receptor, which was promoted by Ser residue (Cui et al., 2024; Guo, Ren, et al., 2024). Guo, Ren, et al. (2024) identified Asn150 residue as a critical site in the binding region of T1R1 subunit due to its high interaction frequency, and the residues of Ser170, Glu301, and Gln389 within T1R3 subunit were also frequently involved in the interactions. More specifically, Ser, Gln, Ala, and Glu residues were prominently represented, collectively accounting for over 50 % of the identified binding sites, particularly the highest occurrence frequency of Ser residue (More than 23 %) (Guo, Ren, et al., 2024). Therefore, the vital binding sites responsible for supplying hydrogen atoms to form hydrogen bonds were residues of Ser109, Asn150, and Ser217 in T1R1 subunit, along with residues of Lys155 and Ser224 in T1R3 subunit. Besides, the vital binding sites supplying oxygen atoms for hydrogen bonds were residues of Ser107, Ser217, and Asp243 in T1R1 subunit, as well as residues of Glu217 and Glu240 in T1R3 subunit.

In addition, statistical analysis classified the binding modes of 224 umami peptides to T1R1/T1R3 receptor into three distinct categories: Mode ① binding to the T1R1 subunit cavity, mode ② embedding into the binding pocket of the cavity of T1R3 subunit, and mode ③ simultaneous interaction with both subunits, which was consistent with the previous report (Guo, Ren, et al., 2024). Within the structure of T1R1/T1R3 receptor, the T1R1 subunit binding cavity maintains a closed conformation, whereas the T1R3 subunit cavity adopts an open state capable of accommodating umami peptide (Fig. 3(A)). Hence, the umami peptides primarily interacted with T1R1/T1R3 receptors through ② and ③ binding modes. Notably, the key docking sites were predominantly situated within the cavity of T1R1/T1R3 receptor, which constituted the venus flytrap domain. These findings aligned with previous reports demonstrating that umami peptides similarly bound to the venus flytrap domain of the receptor *via* hydrogen bonds (Chen et al., 2025).

3.7. Correlation analysis of the intermolecular interactions between umami peptides and T1R1/T1R3 receptor

The intermolecular interactions between umami peptides and the T1R1/T1R3 receptor were systematically summarized in Fig. 7(A–F) and S2. It was evident that polar amino acid residues exhibited a strong propensity to form ionic and hydrogen bonds. For instance, alkaline amino acid residues predominantly contributed to cations and hydrogen atoms, whereas acidic amino acid residues tended to provide anions and oxygen atoms, which were essential for the formation of ionic and hydrogen bonds, respectively. In addition to hydrophobic bonds, hydrophobic amino acid residues also served as significant contributors of hydrogen atoms during hydrogen bond formation. These findings were consistent with the analysis illustrated in Fig. 6.

Moreover, T1R1 and T1R3 subunits played critical roles in chemical bonds, which attributed to umami peptides with similar structures, allowing them to greatly interact with the same region of T1R1/T1R3 receptor. Hence, the vast majority of umami peptides were docked to two subunits of T1R1/T1R3 receptor, especially umami peptides with more than seven amino acid residues. Furthermore, compared to ionic, hydrophobic and hydrogen bonds constituted the primary intermolecular forces driving the interactions between umami peptides and T1R1/T1R3 receptor, but these bonds varied in the key binding sites. Yu et al. (2024) indicated that hydrogen bonds were identified as the primary interaction forces between the umami peptides and T1R1/T1R3 receptor, with key amino acid residues of Tyr198, Ser112, His111, Asn173,

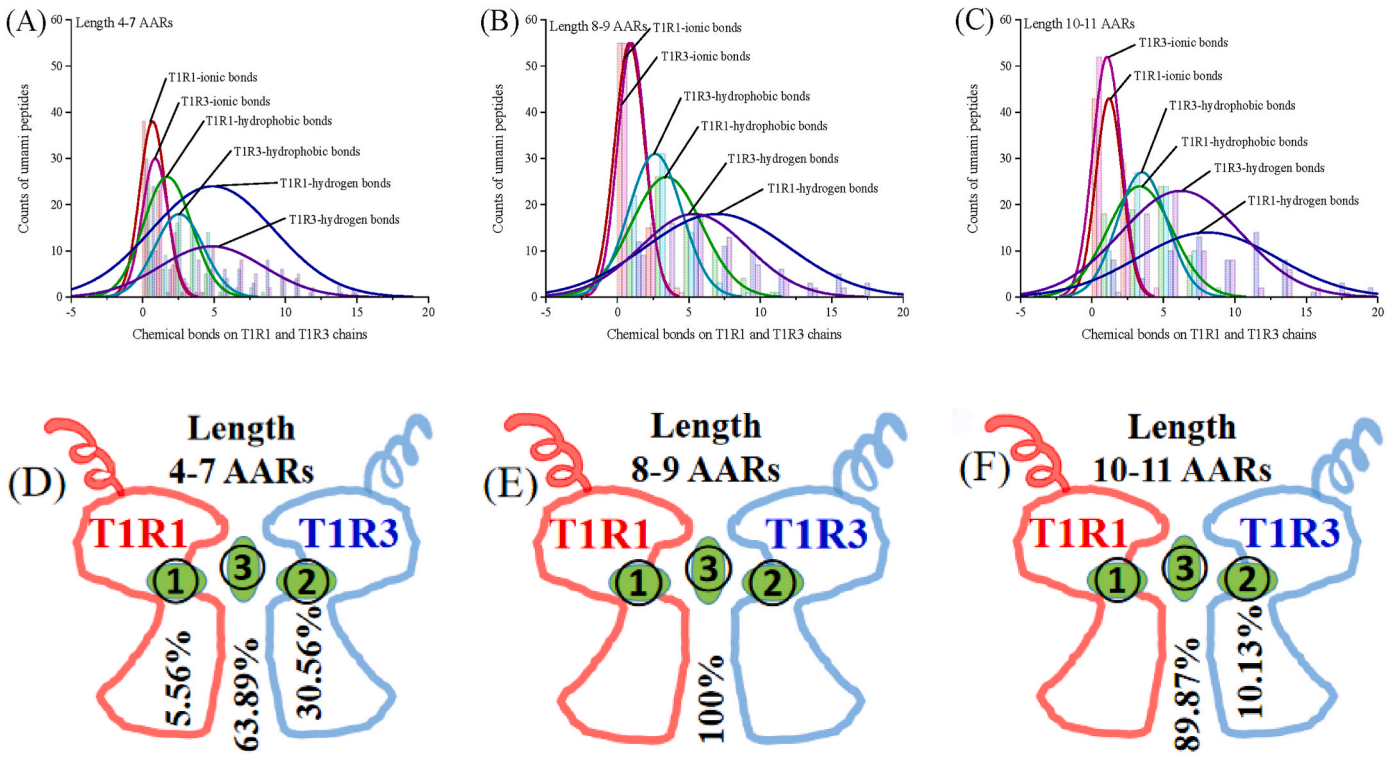

Fig. 7. The summary of key sites connecting to form chemical bonds. (A) Distributions of chemical bond on T1R1 (A chain) and T1R3 (B chain) subunits (umami peptides with 4–7 amino acid residues), (B) distributions of chemical bond on T1R1 and T1R3 subunits (umami peptides with 8–9 amino acid residues), (C) distributions of chemical bond on T1R1 and T1R3 subunits (umami peptides with 10–11 amino acid residues), (D) statistics of docking sites of umami peptides (4–7 amino acid residues) on T1R1/T1R3 receptor, (E) statistics of docking sites of umami peptides (8–9 amino acid residues) on T1R1/T1R3 receptor, (F) statistics of docking sites of umami peptides (10–11 amino acid residues) on T1R1/T1R3 receptor.

and Glu233. Yang et al. (2025) also emphasized that hydrophobic and hydrogen bonds were critical forces to drive the interactions, with the vital binding sites of Glu217, Glu148, Asp216, and His145 residues within T1R1/T1R3 receptor. As a result, through analyzing the interactions between 224 umami peptides and T1R1/T1R3 receptor, it could be concluded that the key binding sites where T1R1/T1R3 receptor interacted with umami peptides *via* hydrophobic and hydrogen bonds. Specifically, the key binding sites were identified as residues of Leu51, Ser107, Ser109, Asp243, and Ile244 in T1R1 subunit, along with the residues of Leu173, Glu217, Arg220, Ser224, and Glu240 in T1R3 subunit.

3.8. Verification of the taste mechanism of umami peptides

3.8.1. Microstructure of interaction between T1R3 receptor and umami peptides

To characterize the binding interactions between the T1R1/T1R3 receptor and umami peptides, the structural changes in the T1R3 receptors were analyzed based on their roughness. Subsequently, before and after exposure to MSG and umami peptides, the two- and three-dimensional structure surface topographies of the T1R3 receptor were compared, as shown in Fig. 8. The T1R3 receptor exhibited a smooth morphological structure with minimal surface roughness (Ra = 0.241 nm, Rq = 0.345 nm; Fig. 8(A)). Following MSG binding, T1R3 receptor might undergo aggregation to significantly increase surface roughness (Fig. 8(B)). Moreover, due to their structural similarity to MSG and larger molecular volume, umami peptides were more prone to induce receptor aggregation (Chang et al., 2024; Song, Wang et al., 2025). As a result, T1R3 receptor surface roughness increased substantially upon binding to umami peptides, particularly the LALDWLAR-receptor complex which exhibited the most pronounced changes in surface topography, reaching maximum roughness values of 0.498 nm (Ra) and 0.740 nm (Rq) [Fig. 8(C–G)]. Notably, these flavor compounds significantly altered T1R3 receptor's vertical profile and surface topography, with umami peptides producing the more pronounced surface topography. The more dramatic structural changes induced by umami peptides suggested localized receptor aggregation and specific ligand-protein interactions (Sun et al., 2025). These findings were consistent with previous reports demonstrating that sulfur-containing flavor compounds increased the height and surface roughness of pea protein isolate, due to inducing protein aggregation and molecular interactions (Sun et al., 2025). These interactions likely facilitated the assembly of new complexes through non-covalent bonds, including hydrogen bonds, hydrophobic bonds and so on (Liang et al., 2024; Sun et al., 2025). This study offers direct visual confirmation of surface morphological alterations of flavor receptor induced by flavor compounds, corroborating mechanistic insights into protein-flavor compound interactions.

3.8.2. Thermodynamic analysis between T1R3 receptor and umami peptides

Comprehensive thermodynamic analysis offered mechanistic insights into the binding behavior of the receptors with umami peptides (Li et al., 2024; Sun et al., 2025), with the thermodynamic parameters revealed in Fig. 9 and Table 1. During the interaction between receptors and flavor compounds, the predominant interaction forces were classified based on thermodynamic signatures: hydrogen bonds and van der Waals forces (Characterized by $\Delta H < 0$ and $\Delta S < 0$), hydrophobic bonds (Characterized by $\Delta H > 0$ and $\Delta S > 0$), and electrostatic interactions (Characterized by $\Delta H < 0$ and $\Delta S > 0$) (Song, Zhao et al., 2025; Sun et al., 2025). The thermodynamic interaction between the T1R3 receptor and umami peptides was spontaneous and exothermic. This was evidenced by the negative Gibbs free energy ($\Delta G < 0$) and reaction heat ($\Delta Q < 0$) values observed for all four umami peptides and MSG binding to the receptor. The spontaneous reaction helped to form new chemical

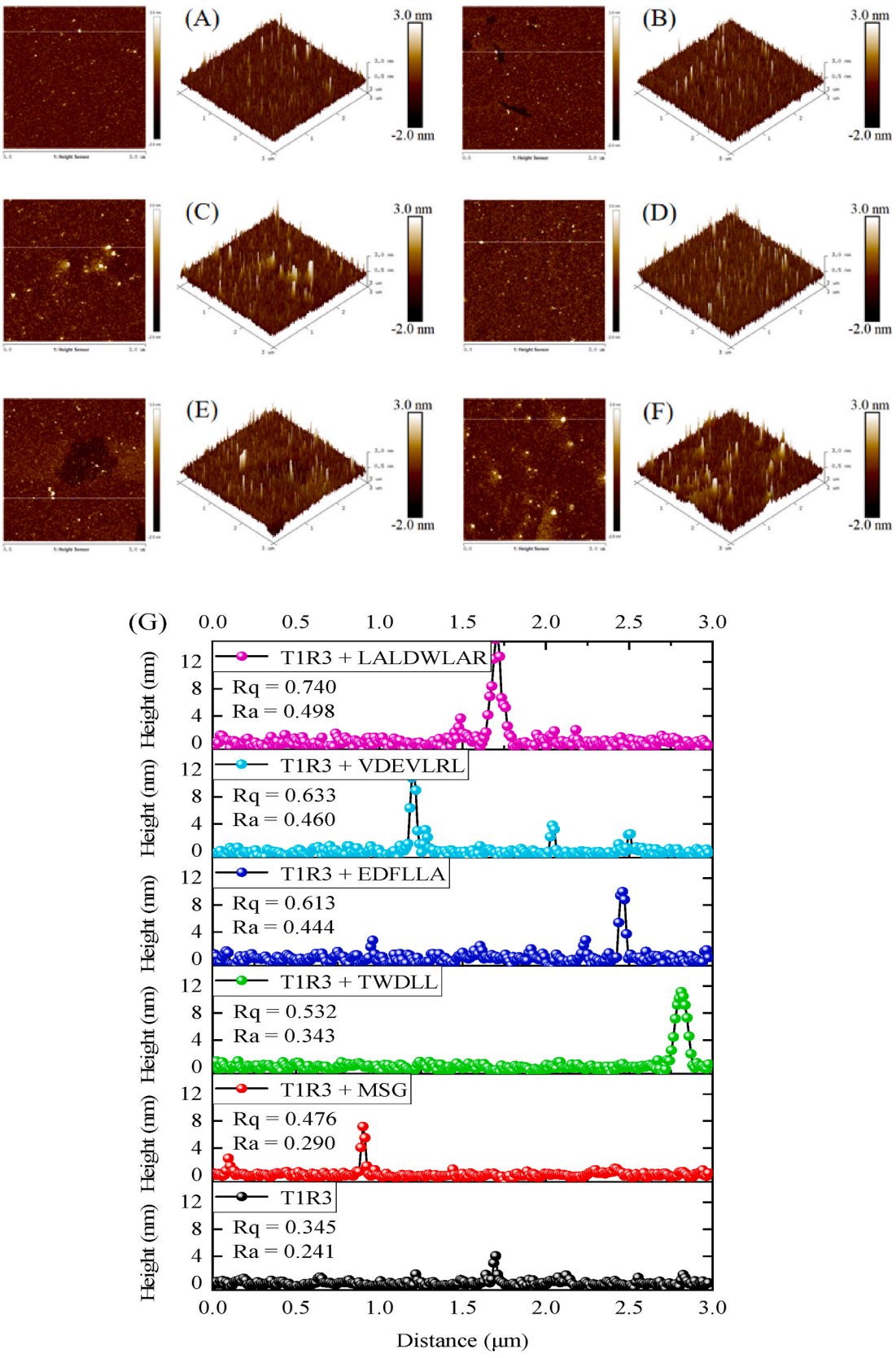

Fig. 8. Atomic force microscopy images of T1R3 receptor and its interactions with monosodium glutamate and umami peptides. (A) T1R3 receptor, (B) T1R3 receptor−monosodium glutamate, (C) T1R3 receptor−TWDLL, (D) T1R3 receptor−EDFLLA, (E) T1R3 receptor−VDEVLRL, (F) T1R3 receptor−LALDWLAR, (G) their average roughness.

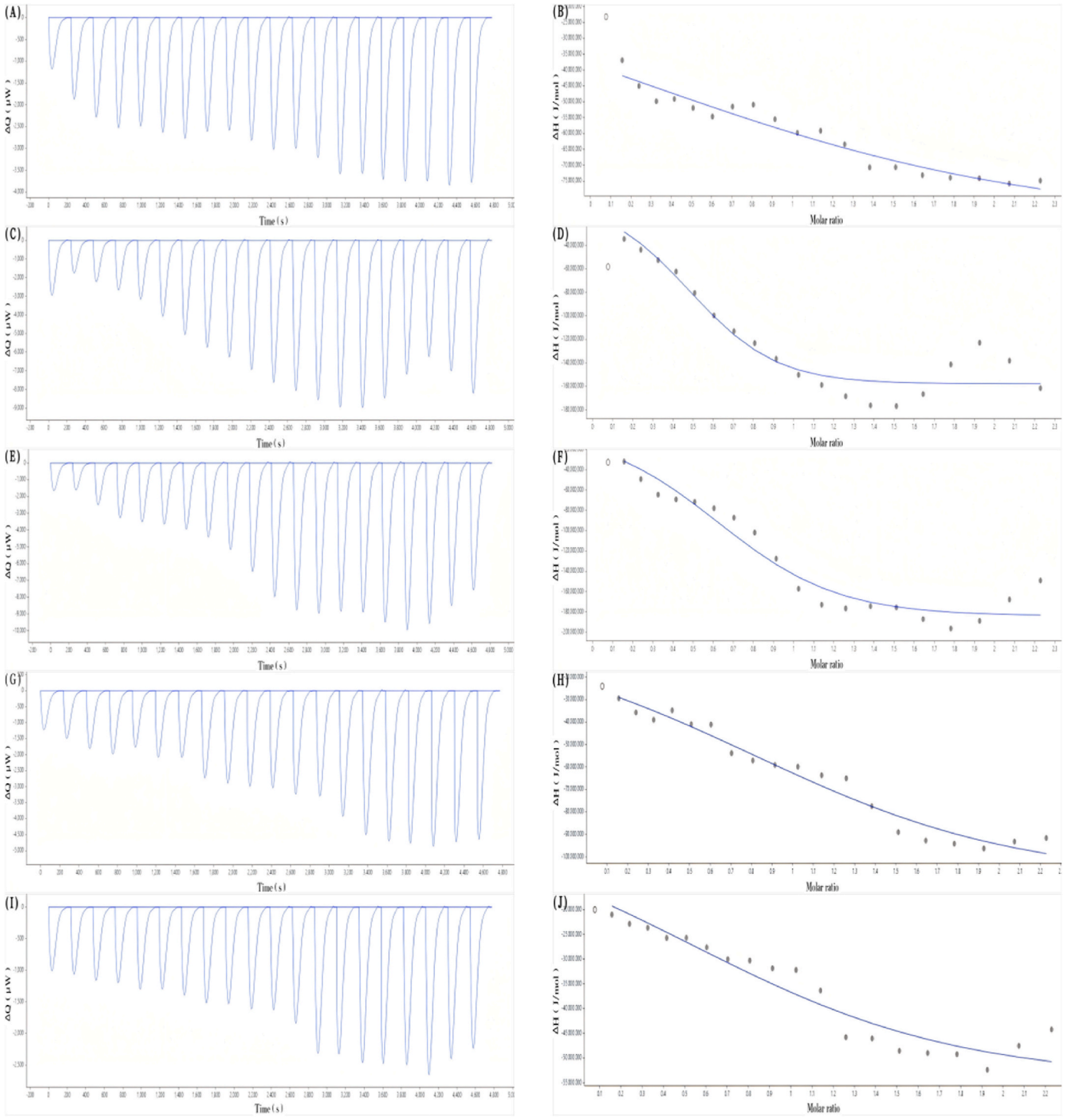

Fig. 9. Molecular thermodynamic diagram of T1R3 receptor interacting with monosodium glutamate and umami peptides. (A–B) Monosodium glutamate, (C–D) TWDLL, (E–F) EDFLLA, (G–H) VDEVLRL, (I–J) LALDWLAR.

bonds within the umami peptide-receptor complexes, which was driven by four vital forces, including hydrophobic bonds, hydrogen bonds, van der Waals forces, and electrostatic interactions (Prozeller et al., 2019). Moreover, the enthalpy (ΔH) and entropy (ΔS) changes were both negative, indicating that the thermodynamic interactions between the T1R3 receptor and umami peptides were enthalpy-driven and involved non-covalent binding. Additionally, the primary binding forces responsible for these interactions were hydrogen bonds and van der Waals forces. Consistent with previous studies (Li et al., 2024), TRPV1 receptor primarily bound to salty peptides driven by hydrogen bonds, aligning with the results of this experiment. Sun et al. (2025) reported that hydrogen bonds contribute to enhancing the stability of pea protein isolate when bound to sulfur- or nitrogen-containing heterocyclic flavor compounds. Guo, Gong et al., 2024 also emphasized that pea protein isolate mainly bound to pyrazine heterocyclic flavor compounds through hydrogen bonds and van der Waals forces. Combining the results of molecular docking, hydrogen bonds contributed to enhancing the stability of T1R1/T1R3 receptor when bound to umami peptides.

All four umami peptides were similar to MSG with the same binding characteristics which could strongly interact with the umami receptor.

Table 1
Parameters of the interaction between umami peptides and the umami receptor and their standard curves of umami characteristics.

Parameter	Monosodium glutamate and umami peptides				
	Monosodium glutamate	TWDLL	EDFLLA	VDEVLRL	LALDWLAR
Fit index (R^2)	0.942	0.917	0.936	0.962	0.916
ΔG (kJ/mol)	−41.94	−47.17	−46.74	−43.55	−41.85
Reaction heat ΔQ (μW)	−57074.96	−115461.57	−121381.60	−60753.83	−34504.79
ΔH (kJ/mol)	−35661.72	−129527.93	−151563.42	−69543.18	−31460.51
$T\Delta S$ (kJ/mol)	−35619.78	−129480.76	−151516.67	−69499.63	−31418.65
Ka (M^{-1})	22237685	183813214	154582057	42634412	21491139
Kd (M)	4.496×10^{-8}	5.440×10^{-9}	6.469×10^{-9}	2.345×10^{-8}	4.653×10^{-8}
Junction site (n)	0.2565	0.4836	0.6257	0.8101	0.5321
Standard curves	Y = 3.9351x+2.8452	Y = 4.5496x−0.8610	Y = 4.6462x−1.1697	Y = 4.6088x−1.0979	Y = 4.1276x−1.2828
R^2	0.9393	0.9579	0.9354	0.9289	0.9277

This was evidenced by the binding affinity constants (Kd) ranging from 5.440×10^{-9} to 4.653×10^{-8} M. More specifically, the lowest binding affinity constants (Kd) identified TWDLL as the most potent ligand for the T1R3 receptor, suggesting optimal molecular complementarity, followed by EDFLLA. Moreover, owing to their small molecular volume, short-chain umami peptides encounter minimal steric hindrance, enabling efficient penetration into the T1R3 receptor's binding pocket and subsequent interaction with its binding sites (Hu et al., 2024; Xie et al., 2024). This structural advantage promoted the formation of stable peptide-T1R3 receptor complexes characterized by low binding affinity constants (Kd) (Hu et al., 2024; Xie et al., 2024). These results accounted for the binding affinity constants (Kd) of umami peptides increasing with peptide chain length. Molecular thermodynamics diagram of four peptides interacted with the TRPV1 receptors ranging from 1.353×10^{-8} to 9.775×10^{-5} M (Li et al., 2024).

In addition, the junction site values (n) for the four umami peptides ranged from 0.4836 to 0.8101, indicating binding stoichiometries generally varying from 2:1 to 1:1 (T1R3 receptor:peptide). Although long-chain umami peptides possess multiple potential binding sites for the receptor, their binding stoichiometries are primarily determined by the binding modes. More specifically, VDEVLRL can simultaneously interact with both subunits [Binding mode ③, referred to Fig. 4(C)], resulting in a 1:1 binding ratio with T1R3 as evidenced by its high junction site value. However, the three remaining umami peptides (TWDLL, EDFLLA, and LALDWLAR) can embed into the binding pocket of the cavity of T1R3 subunit (Binding mode ②, referred to Fig. 4), which causes a receptor-to-peptide binding ratio of 2:1 due to their low junction site values. Moreover, the stoichiometric number of receptor-ligand binding is actually affected by many factors, including the ionic strength and pH value of the system (Liang et al., 2024; Zou et al., 2019). EGCG binds to myosin with a stoichiometry of approximately 4:1 (EGCG:myosin) under high ionic strength conditions (0.5 M NaCl), which decreases to 2:1 at lower ionic strength (0.2 M NaCl) (Liang et al., 2024). This salt-dependent behavior suggests that ionic strength modulates the accessibility of ligand binding sites on the receptor. The stoichiometry values (n = 0.139, 0.021, and 0.105) were measured at pH 3.2, 4.5, and 7.0, respectively, and also demonstrated pH-dependent binding ratios between soy protein isolate (Rreceptor) and grape seed procyanidins (Ligand) (Zou et al., 2019).

3.8.3. *Taste characteristics of synthetic umami peptides*

The umami taste profiles of four umami peptides (TWDLL, EDFLLA, VDEVLRL, and LALDWLAR) were quantitatively analyzed and presented in Fig. 10(A–B). All four umami peptides exhibited pronounced umami characteristics with strong taste intensities and high sensory scores. Notably, although LALDWLAR demonstrated relatively a lower umami intensity compared to the other umami peptides, it still maintained significant umami potential, more than 47 % of the umami intensity observed in an equal concentration of MSG. The result was consistent with the findings which that the MSG concentration corresponding to 50 % selectivity was calculated as the equivalent umami intensity of the umami peptide (Yang et al., 2024). Compared to LALDWLAR, the three remaining umami peptides (TWDLL, EDFLLA, and VDEVLRL) demonstrated remarkable umami characteristics, exhibiting strong taste intensities and high sensory scores. But uammai characteristics of the peptides were lower than that of MSG. Furthermore, we also observed an inverse correlation between peptide chain length and umami characteristics. Specifically, both taste intensity and sensory score decreased with the extension of peptide chain length, which was consistent with the predicted results in Fig. 2. Peptide taste perception is governed by multiple structural factors, notably molecular size, amino acid types and arrangement, and spatial structure of the peptides (Song, Zhao et al., 2025; Yang et al., 2024). According to their umami standard curves (With high slope), the umami characteristics of umami peptides were highly dependent on their concentrations (Table 1).

Sensory evaluation of the four typical umami peptides revealed distinct clustering patterns in principal component analysis (PCA). While the primary variation was observed along PC1, minor differentiation was detected in PC2. The results consistently demonstrated strong umami intensity different from MSG, which was in agreement with previously reported. For instance, four novel umami peptides (RPPVVR, APDFGNR, RGFGGAR, and SWLDGK) exhibited a strong ability of

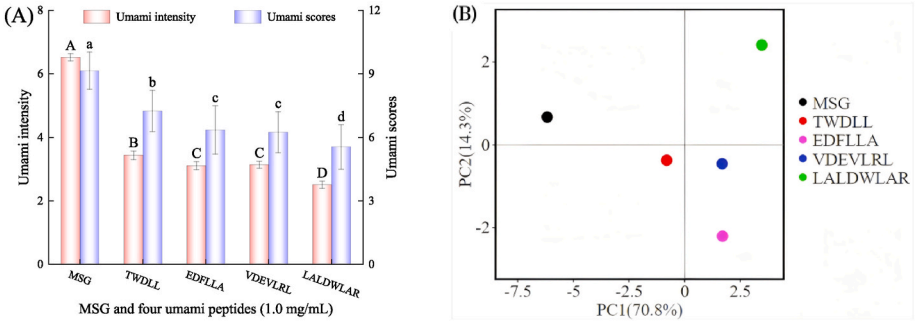

Fig. 10. The umami intensities and scores of umami peptides. (A) Umami intensities and scores, (B) PCA analysis of sensory scores.

umami taste, with the thresholds ranging from 0.27 to 0.48 mg/mL (Chang et al., 2024). The umami peptides KAELDLH, LKEAHDVA, and LGKSEDDVSK also had strong umami activity, with the umami taste thresholds of 0.15, 0.28, and 0.23 mM, respectively, which were lower than those of 0.5 mg/mL MSG solution (Chen et al., 2025). As a result, these findings demonstrated that the integrated approach combining peptidomic and molecular docking was a reliable strategy for identifying potential umami peptides. In particular, the identified peptides showed promising potential as effective sodium substitutes in the development of reduced-sodium food products.

4. Conclusion

In conclusion, this study successfully identified 224 umami peptides from *M. lyrata* hydrolysates, with peptide chain length ranging from 4 to 11 amino acid residues, which was the ideal length for umami peptides. These umami peptides were abundant in acidic amino acid residues. In particular, most N- and C-terminals were predominantly occupied by hydrophobic and polar amino acid residues, which caused the acidic amino acids and their related segments to become vital umami sequences of umami peptides. Furthermore, umami peptides might form intramolecular chemical bonds within the peptides, including ionic, hydrophobic, and hydrogen bonds under the influence of T1R1/T1R3 receptor. Moreover, umami peptides induced significant conformational changes in the T1R3 receptor, as evidenced by increased surface roughness. Integrated analysis of thermodynamic parameters, umami attributes, and molecular docking demonstrated that the receptor-peptide complex was predominantly mediated by hydrogen and hydrophobic bonds, exhibiting an average binding energy of −7.4 kcal/mol. More specifically, the key binding sites were identified as residues of Leu51, Ser107, Ser109, Asp243, and Ile244 in T1R1 subunit, along with the residues of Leu173, Glu217, Arg220, Ser224, and Glu240 in T1R3 subunit. Consequently, these findings established a novel methodology and comprehensive analytical framework for quickly screening umami peptides from complex food systems. The elucidated structure-taste relationships significantly provide critical insights into umami taste perception, particularly integrating computational peptide screening with experimental validation of taste receptor interactions. However, the precise binding sites within T1R1/T1R3 receptor for umami peptides should require experimental confirmation, such as knocking out or modifying the binding active sites for further re-docking. Furthermore, future studies should focus on umami peptides potential interactions with other taste receptors and how umami signal transduction, which can develop umami peptides as food-derived seasoning ingredients, replacing MSG in low-sodium food.

CRediT authorship contribution statement

Chunyong Song: Writing – review & editing, Writing – original draft, Methodology, Investigation. **Rong Jiang:** Data curation, Conceptualization. **Mingtang Tan:** Methodology, Formal analysis. **Zhongqin Chen:** Software, Resources. **Huina Zheng:** Supervision, Software. **Jialong Gao:** Visualization, Validation. **Haisheng Lin:** Visualization, Validation. **Wenhong Cao:** Writing – review & editing, Project administration, Methodology, Funding acquisition.

Ethical statement

We confirm that the appropriate protocols for protecting the rights and privacy of all participants were followed in the execution of the sensory evaluation.

Declaration of competing interest

☑The authors declare that they have no known competing financial interests or personal relationships that could have appeared to influence the work reported in this paper.

Acknowledgments

This work was supported by the Shenzhen Science and Technology Program (JCYJ20230807120316033) and the Modern Agricultural Industry Technology Research System of China (CARS-49). We gratefully acknowledge the anonymous referees for the comments and constructive suggestions provided for improving the manuscript.

Appendix A. Supplementary data

Supplementary data to this article can be found online at https://doi.org/10.1016/j.fbio.2025.107412.

Data availability

Data will be made available on request.

References

Amin, M. U. G., Kusnadi, J., Hsu, J. L., Doerksen, R. J., & Huang, T. C. (2020). Identification of a novel umami peptide in tempeh (Indonesian fermented soybean) and its binding mechanism to the umami receptor T1R. *Food Chemistry, 333*. https://doi.org/10.1016/j.foodchem.2020.127411

Cao, K. X., An, F. Y., Wu, J. R., Ji, S. Q., Rong, Y. Z., Hou, Y. C., Ma, X. W., Yang, W. X., Hu, L. K., & Wu, R. N. (2023). Identification, characterization, and receptor binding mechanism of new umami peptides from traditional fermented soybean paste (Dajiang). *Journal of Agricultural and Food Chemistry, 71*(48), 18953–18962. https://doi.org/10.1021/acs.jafc.3c04943

Chang, L. Y., Zhang, X. Z., Zhang, Z. Q., Cai, F. Y., Yu, H., Lin, D., Liu, H. M., & Zhao, Q. (2024). Isolation and characterization of novel umami peptides from bay scallop (*Argopecten irradians*) and molecular docking to the T1R1/T1R3 taste receptor. *LWT-Food Science and Technology, 207*, Article 116645. https://doi.org/10.1016/j.lwt.2024.116645

Chen, D. Y., Rong, M. L., Tang, S. T., Zhang, C. X., Wei, H., Yuan, Z. T., Miao, T. W., Song, H. C., Jiang, H. M., Yang, Y., & Zhang, L. J. (2025). A novel directed enzymolysis strategy for the preparation of umami peptides in *Stropharia rugosoannulata* and its mechanism of taste perception. *Food Chemistry, 468*, Article 142385. https://doi.org/10.1016/j.foodchem.2024.142385

Cui, Z. Y., Meng, H. L., Zhou, T. X., Yu, Y. Y., Gu, J. M., Zhang, Z. W., Zhu, Y. W., Zhang, Y., Liu, Y., & Wang, W. L. (2024). Noteworthy consensus effects of D/E residues in umami peptides used for designing the novel umami peptides. *Journal of Agricultural and Food Chemistry, 72*(5), 2789–2800. https://doi.org/10.1021/acs.jafc.3c07026

Fu, B. F., Li, M. B., Chang, Z. H., Yi, J. J., Cheng, S. Z., & Du, M. (2025). Identification of novel umami peptides from oyster hydrolysate and the mechanisms underlying their taste characteristics using machine learning. *Food Chemistry, 473*, Article 142970. https://doi.org/10.1016/j.foodchem.2025.142970

Guo, Y. N., Gong, Q., Sun, F. W., Cheng, T. F., Fan, Z. J., Huang, Z. X., Liu, J., Guo, Z. W., & Wang, Z. J. (2024). Interaction mechanism of pea proteins with selected pyrazine flavors: Differences in alkyl numbers and flavor concentration. *Food Hydrocolloids, 147*, Article 109314. https://doi.org/10.1016/j.foodhyd.2023.109314

Guo, W. D., Ren, K. Z., Long, Z., Fu, X. J., Zhang, J. N., Liu, M., & Chen, Y. Q. (2024). Efficient screening and discovery of umami peptides in Douchi enhanced by molecular dynamics simulations. *Food Chemistry X, 24*, Article 101940. https://doi.org/10.1016/j.fochx.2024.101940

Guo, J., Yu, X. J., Zhou, C. S., Wang, B., Zhang, L., Otu, P., Chen, L., Niu, Y. W., Yao, D. Y., Hua, C. H., & Ma, H. L. (2024). Preparation of umami peptides from chicken breast by ultrasound-assisted gradient dilution feeding substrate and study of their formation mechanism. *Food Bioscience, 62*, Article 105176. https://doi.org/10.1016/j.fbio.2024.105176

Han, A. P., Liu, H. S., Dai, Y. X., Sun, S. G., & Ma, H. J. (2024). Screening of umami peptides from fermented grains by machine learning, molecular docking and molecular dynamics simulation. *Food Bioscience, 62*, Article 105536. https://doi.org/10.1016/j.fbio.2024.105536

Hiranpradith, V., Therdthai, N., & Soontrunnarudrungsri, A. (2023). Effect of steaming and microwave heating on taste of clear soup with split-gill mushroom powder. *Foods, 12*(8), 1685. https://doi.org/10.3390/foods12081685

Hossain, M. Y., Uddin, M., Rahman, M. A., Haque, M. K., Kormoker, T., Samad, M. A., Tanjin, S., Rahman, M. A., Parvin, M. F., Sarmin, M. S., Mawa, Z., Habib, K. A., Rahman, M. S., Tasmin, R., Yeasmin, S., Mahmud, Y., Idris, A. M., Al-Qthanin, R. N., & Tsang, Y. F. (2023). Species identification, reproductive biology, and nutritional value of marine shellfish (*Meretrix lyrata*) in the Bay of Bengal. *Marine Environmental Research, 192*, Article 106222. https://doi.org/10.1016/j.marenvres.2023.106222

Hu, Y. Y., Badar, I. H., Liu, Y., Zhu, Y., Yang, L. W., Kong, B. H., & Xu, B. C. (2024). Advancements in production, assessment, and food applications of salty and saltiness-enhancing peptides: A review. *Food Chemistry, 453*, Article 139664. https://doi.org/10.1016/j.foodchem.2024.139664

Jia, R., Yang, Y., Liao, G. Z., Wu, H. Y., Yang, C. F., & Wang, G. Y. (2024). Flavor characteristics of umami peptides from Wuding chicken revealed by molecular dynamics simulation. *Journal of Agricultural and Food Chemistry, 72*(7), 3673–3682. https://doi.org/10.1021/acs.jafc.3c08348

Kong, C. M., Pan, T., Chen, X. K., Junaid, M., Liao, H. P., Gao, D. D., Wang, Q. P., Liu, W. J., Wang, X., & Wang, J. (2023). Exposure to polystyrene nanoplastics and PCB77 induced oxidative stress, histopathological damage and intestinal microbiota disruption in white hard clam *Meretrix lyrata*. *Science of The Total Environment, 905*, Article 167125. https://doi.org/10.1016/j.scitotenv.2023.167125

Le, B., Yu, B. B., Amin, M. S., Liu, R. X., Zhang, N., Soladoye, O. P., Aluko, R. E., Zhang, Y. H., & Fu, Y. (2022). Salt taste receptors and associated salty/salt taste-enhancing peptides: A comprehensive review of structure and function. *Trends in Food Science & Technology, 129*, 657–666. https://doi.org/10.1016/J.TIFS.2022.11.014

Lee, D., Kim, H. J., & Jo, C. (2025). Novel umami-enhancing peptides of beef *M. Semimembranosus* hydrolysates and interactions with the T1R1/T1R3 taste receptor. *Food Chemistry, 463*(3), Article 141368. https://doi.org/10.1016/j.foodchem.2024.141368

Li, Z. Q., Shi, K., Xue, L. X., Zhang, Y., Song, H. L., Liao, Y. C., Shi, H., & Shi, W. F. (2025). Characterization and molecular docking study of umami peptides from *Agaricus bisporus* and *Volvariella volvacea* by sensory analysis combined with UPLC-ESI-Q-TOF MS. *Journal of Food Composition and Analysis, 140*, Article 107200. https://doi.org/10.1016/j.jfca.2025.107200

Li, W., Sun, S., Chen, W. C., Ma, H. L., Li, T. Z., Zhang, Z., Wu, D., Yan, M. Q., & Yang, Y. (2024). Exploring the taste presentation and receptor perception mechanism of salty peptides from *Stropharia rugosoannulata* based on molecular dynamics and thermodynamics simulation. *Food Science and Human Wellness, 13*(4), 2277–2288. https://doi.org/10.26599/FSHW.2022.9250190

Liang, J. J., Chen, X. J., Majura, J. J., Tan, M. T., Chen, Z. Q., Gao, J. L., & Cao, W. H. (2025). Insight into the structure-activity relationship of thermal hysteresis activity of cod collagen peptides through peptidomics and bioinformatics approaches. *Food Chemistry, 463*(4), Article 141514. https://doi.org/10.1016/j.foodchem.2024.141514

Liang, Q. Q., Zhang, X. H., Jiang, X., Pan, D., Zhang, Z., Bai, Z. Y., & Shi, W. Z. (2024). The mechanism underlying increased myosin solubility in pearl mussels (*Hyriopsis cumingii*) by epigallocatechin gallate at low NaCl level. *Food Bioscience, 58*, Article 103692. https://doi.org/10.1016/j.fbio.2024.103692

Lindemann, B. (2001). Receptors and transduction in taste. *Nature, 413*, 219–225. https://doi.org/10.1038/35093032

Prozeller, D., Morsbach, S., & Landfester, K. (2019). Isothermal titration calorimetry as a complementary method for investigating nanoparticle-protein interactions. *Nanoscale, 11*(41), 19265–19273. https://doi.org/10.1039/C9NR05790K

Rapino, F., Zhou, Z. L., Sanchez, A. M. R., Joiret, M., Seca, C., Hachem, N. E., Valenti, G., Latini, S., Shostak, K., Geris, L., Li, P., Huang, G., Mazzucchelli, G., Baiwir, D., Desmet, C. J., Chariot, A., Georges, M., & Close, P. (2021). Wobble tRNA modification and hydrophilic amino acid patterns dictate protein fate. *Nature Communications, 12*(1), 2170. https://doi.org/10.1038/s41467-021-22254-5

Roper, S. D., & Chaudhari, N. (2017). Taste bud: Cells, signals and synapses. *Nature Reviews Neuroscience, 18*(8), 485–497. https://doi.org/10.1038/nrn.2017.68

Song, C. Y., Wang, Z. J., Li, H. Q., Cao, W. H., Chen, Z. Q., Zheng, H. N., Gao, J. L., Lin, H. S., & Zhu, G. P. (2025). Recent advances in taste transduction mechanism, analysis methods and strategies employed to improve the taste of taste peptides. *Critical Reviews in Food Science and Nutrition, 65*(4), 695–714. https://doi.org/10.1080/10408398.2023.2280246

Song, C. Y., Yang, Y. F., Zhao, Z. H., Tan, M. T., Chen, Z. Q., Zheng, H. N., Gao, J. L., Lin, H. S., Zhu, G. P., & Cao, W. H. (2024). Insight into the correlation of taste substances and salty-umami taste from *Monetaria moneta* hydrolysates prepared using different proteases. *Food Chemistry X, 24*, Article 102056. https://doi.org/10.1016/j.fochx.2024.102056

Song, C. Y., Zhao, Z. H., Tan, M. T., Chen, Z. Q., Zheng, H. N., Gao, J. L., Lin, H. S., Qin, X. M., & Cao, W. H. (2025). Screening of salty peptides from enzymatic hydrolysates of *Meretrix lyrata* based on interaction with the TMC4 receptor. *Food Research International, 218*, Article 116930. https://doi.org/10.1016/j.foodres.2025.116930

Sun, H. L., Liang, J. Y., Qian, Y. R., Chen, X., & Zhao, L. Y. (2025). Interactions of pea protein with three sulfur-containing flavor compounds: Insights into molecule structural, non-covalent, and binding mechanisms. *Food Hydrocolloids, 166*, Article 111326. https://doi.org/10.1016/j.foodhyd.2025.111326

Wang, J., Huang, X. H., Zhang, Y. Y., Li, S. J., Dong, X. P., & Qin, L. (2023). Effect of sodium salt on meat products and reduction sodium strategies-A review. *Meat Science, 205*, Article 109296. https://doi.org/10.1016/j.meatsci.2023.109296

Xie, X. N., Dang, Y. L., Pan, D. D., Nawazish, H., Li, Y., & Gao, X. C. (2024). Screening of novel umami peptides with saltiness enhancement effect using molecular docking and structure-activity analysis. *Food Research International, 197*(1), Article 115208. https://doi.org/10.1016/j.foodres.2024.115208

Yan, J. N., & Tong, H. R. (2022). An overview of bitter compounds in foodstuffs: Classifications, evaluation methods for sensory contribution, separation and identification techniques, and mechanism of bitter taste transduction. *Comprehensive Reviews in Food Science and Food Safety, 22*(1), 187–232. https://doi.org/10.1111/1541-4337.13067

Yang, C. H., Ge, X. H., Ge, C. R., Zhao, P., Liang, S. M., & Xiao, Z. C. (2025). Taste characterization and molecular docking study of novel umami flavor peptides in Yanjin black bone chicken meat. *Food Chemistry, 464*(2), Article 141695. https://doi.org/10.1016/j.foodchem.2024.141695

Yang, J., Huang, Y. R., Cui, C., Dong, H., Zeng, X. F., & Wei, W. D. (2021). Umami-enhancing effect of typical kokumi-active γ-glutamyl peptides evaluated *via* sensory analysis and molecular modeling approaches. *Food Chemistry, 338*, Article 128018. https://doi.org/10.1016/j.foodchem.2020.128018

Yang, F., Lv, S., Liu, Y., Bi, S., & Zhang, Y. (2022). Determination of umami compounds in edible fungi and evaluation of salty enhancement effect of *Antler fungus* enzymatic hydrolysate. *Food Chemistry, 387*, Article 132890. https://doi.org/10.1016/j.foodchem.2022.132890

Yang, F., Meng, H. Y., Fu, A. Z., Liu, Y., & Bi, S. (2024). Quantification-and structural-taste intensity of umami peptides from *Agrocybe aegerita* through quantitative structure-activity relationship. *Food Chemistry, 455*, Article 139919. https://doi.org/10.1016/j.foodchem.2024.139919

Yao, Y. X., Shi, Y. L., Yi, Y. Y., Zhu, J. Q., Kang, Q. Z., Qu, L. B., Yang, R., Lu, J. K., & Zhao, C. C. (2024). Three novel umami peptides from watermelon soybean paste and the revelation of the umami mechanism through molecular docking with T1R1/T1R3. *Food Bioscience, 59*, Article 104155. https://doi.org/10.1016/j.fbio.2024.104155

Yu, Y. Y., Cui, Z. Y., Zhou, T. X., Wang, Y. M., Chen, P. P., Wang, S. N., Zhu, Y. W., Liu, J., Jiang, S., & Liu, Y. (2025). Umami peptide synergy unveiled: A comprehensive study from molecular simulation to practical validation of sensing strategy. *Biosensors and Bioelectronics, 278*, Article 117331. https://doi.org/10.1016/j.bios.2025.117331

Yu, Z. Z., Liu, M. Z., Xu, J., Fan, X. K., Wang, W., Sun, Y. Y., & Pan, D. D. (2024). Rapid screening of novel umami peptides in high-umami scored air-dried chicken under low-salt processing based on molecular sensory techniques. *Food Bioscience, 62*, Article 105479. https://doi.org/10.1016/j.fbio.2024.105479

Zhang, J. C., He, W., Liang, L., Sun, B. G., & Zhang, Y. Y. (2024). Study on the saltiness-enhancing mechanism of chicken-derived umami peptides by sensory evaluation and molecular docking to transmembrane channel-like protein 4 (TMC4). *Food Research International, 182*, Article 114139. https://doi.org/10.1016/j.foodres.2024.114139

Zhang, J. W., Tu, Z. C., Wen, P. W., Wang, H., & Hu, Y. M. (2024). Peptidomics screening and molecular docking with umami receptors T1R1/T1R3 of novel umami peptides from oyster (*Crassostrea gigas*) hydrolysates. *Journal of Agricultural and Food Chemistry, 72*(1), 634–646. https://doi.org/10.1021/acs.jafc.3c06859

Zou, Y. C., Wu, C. L., Ma, C. F., He, S., Brennan, C. S., & Yuan, Y. (2019). Interactions of grape seed procyanidins with soy protein isolate: Contributing antioxidant and stability properties. *LWT-Food Science and Technology, 115*, Article 108465. https://doi.org/10.1016/j.lwt.2019.108465